Review

Materials and Life Science Experimental Facility at the Japan Proton Accelerator Research Complex III: Neutron Devices and Computational and Sample Environments

Kaoru Sakasai [1,*], Setsuo Satoh [2], Tomohiro Seya [2], Tatsuya Nakamura [1], Kentaro Toh [1], Hideshi Yamagishi [3], Kazuhiko Soyama [1], Dai Yamazaki [1], Ryuji Maruyama [1], Takayuki Oku [1], Takashi Ino [2], Hiroshi Kira [4], Hirotoshi Hayashida [4], Kenji Sakai [1], Shinichi Itoh [2], Kentaro Suzuya [1], Wataru Kambara [1], Ryoichi Kajimoto [1], Kenji Nakajima [1], Kaoru Shibata [1], Mitsutaka Nakamura [1], Toshiya Otomo [2], Takeshi Nakatani [1], Yasuhiro Inamura [1], Jiro Suzuki [5], Takayoshi Ito [4], Nobuo Okazaki [4], Kentaro Moriyama [4], Kazuya Aizawa [1], Seiko Ohira-Kawamura [1] and Masao Watanabe [1]

[1] Materials and Life Science Division, J-PARC Center, Japan Atomic Energy Agency (JAEA), Tokai, Ibaraki 319-1195, Japan; nakamura.tatsuya@jaea.go.jp (T.N.); toh.kentaro@jaea.go.jp (K.T.); soyama.kazuhiko@jaea.go.jp (K.So.); dai.yamazaki@j-parc.jp (D.Y.); ryuji.maruyama@j-parc.jp (R.M.); takayuki.oku@j-parc.jp (T.Ok.); kenji.sakai@j-parc.jp (Ke.S.); suzuya.kentaro@jaea.go.jp (K.Su.); kambara.wataru@jaea.go.jp (W.K.); ryoichi.kajimoto@j-parc.jp (R.K.); kenji.nakajima@j-parc.jp (K.N.); shibata.kaoru@jaea.go.jp (K.Sh.); nakamura.mitsutaka@jaea.go.jp (M.N.); takeshi.nakatani@j-parc.jp (T.N.); yasuhiro.inamura@j-parc.jp (Y.I.); aizawa.kazuya@jaea.go.jp (K.A.); seiko.kawamura@j-parc.jp (S.O.-K.); masao.watanabe@j-parc.jp (M.W.)

[2] Institute of Materials Structure Science, High Energy Accelerator Research Organization (KEK), Tsukuba, Ibaraki 300-3256, Japan; setsuo.satoh@kek.jp (S.S.); seyat@post.j-parc.jp (T.S.); takashi.ino@kek.jp (T.In.); shinichi.itoh@kek.jp (S.I.); toshiya.otomo@kek.jp (T.Ot.)

[3] Nippon Advanced Technology, Ltd., Tokai, Ibaraki 319-1106, Japan; yamagishi.hideshi@jaea.go.jp (H.Y.)

[4] Neutron Science and Technology Center, Comprehensive Research Organization for Science and Society (CROSS), Tokai, Ibaraki 319-1106, Japan; h_kira@cross.or.jp (H.K.); h_hayashida@cross.or.jp (H.H.); t_ito@cross.or.jp (T.It.); n_okazaki@cross.or.jp (N.O.); k_moriyama@cross.or.jp (K.M.)

[5] Computing Research Center, High Energy Accelerator Research Organization (KEK), Tsukuba, Ibaraki 300-3256, Japan; jiro.suzuki@j-parc.jp (J.S.)

* Correspondence: sakasai.kaoru@jaea.go.jp; Tel.: +81-29-284-3519

Abstract: Neutron devices such as neutron detectors, optical devices including supermirror devices and ^{3}He neutron spin filters, and choppers are successfully developed and installed at the Materials Life Science Facility (MLF) of the Japan Proton Accelerator Research Complex (J-PARC), Tokai, Japan. Four software components of MLF computational environment, instrument control, data acquisition, data analysis, and a database, have been developed and equipped at MLF. MLF also provides a wide variety of sample environment options including high and low temperatures, high magnetic fields, and high pressures. This paper describes the current status of neutron devices, computational and sample environments at MLF.

1. Introduction

Neutron devices play an important role in the work that goes on at neutron scattering facilities. At the Materials and Life Science Facility (MLF) of the Japan Proton Accelerator Research Complex (J-PARC), we have been developing advanced neutron devices such as neutron detectors, supermirror devices, ^{3}He neutron spin filters, and choppers with high performance at MLF. On the other hand, in a large facility such as MLF, sophisticated computational environment is indispensable for data acquisition (DAQ) and analysis. At MLF, four software components, instrument control, DAQ, data analysis, and a database, have been equipped. Furthermore, the sample environment (SE) is very important for neutron scattering experiments. Therefore, a special SE team is organized to operate, perform maintenance, and develop common SE equipment at MLF. In this paper, the state of the art of neutron devices, computational environment, and sample environment at MLF are described.

2. Neutron Devices

2.1. Neutron Detectors

2.1.1. A Neutron Encode with High Speed Network—(NeuNET) Module for ^{3}He Position Sensitive Detector

Several neutron instruments at MLF require large detector systems that cover very large solid angles and have a high pixel resolution and many time-of-flight (TOF) channels. More than 1000 linear position-sensitive ^{3}He gas detectors (PSDs) are used in instruments at MLF, such as high-resolution powder diffractometers and small-/wide-angle diffractometers. We have developed a new neutron encode with high speed network —(NeuNET) module and a large-scale DAQ system to satisfy the abovementioned requirements of large detector systems; the NeuNET module and DAQ system have an outstanding ability to process a large number of PSD signals. The NeuNET module can process data from PSDs having lengths in the range of 60 cm to 3 m, and it comprises a high-speed network (SiTCP) that lends flexibility and scalability to the DAQ system.

The NeuNET module combines the neutron measurement technology [1] developed at the KEK Neutron Science Laboratory (Tsukuba, Japan) and the network technology [2] developed at the KEK Institute of Particle and Nuclear Studies (Tsukuba, Japan). Figure 1a shows a picture of the NeuNET module. One NeuNET module that comprises one slot and whose height is double that specified by Versa module Europe (VME) standards processes the data of eight PSDs. Figure 1b shows a block diagram of the NeuNET module. When the PSD captures a neutron, the daughter board receives the signals of both sides (left and right) of the PSD, converting neutron signals into digital data via two analog-to-digital converters (ADCs). The field programmable gate array (FPGA) on the board detects the peak of the signal to calculate the pulse height from the difference between the peak and the baseline. If the sum of the pulse heights of the left and right signals exceeds the threshold, the signals are stored as the captured neutron data. The pulse heights and a time stamp at the detected peak are sent to the main FPGA on the main board.

The SiTCP system transfers the data from the NeuNET module to the DAQ system by means of a high-speed network without a CPU. The network is of the 100BASE-TX standard, and can transfer the data at almost the maximum speed (11 Mbyte/s) by the Transmission Control Protocol/Internet Protocol (TCP/IP). A standard PSD generates neutron data 30 k-cps (count per second) at most. Because the NeuNET module transmits the data of eight PSDs, the maximum data rate is 8×30 k-cps $\times 8$ bytes = 1.42 M-byte/s. Therefore, the NeuNET module has a fairly high network capacity. The DAQ system with the NeuNET module is the de facto standard at MLF; it is used in more than half of the experimental spectrometers at this facility and can control thousands of ^{3}He gas detectors.
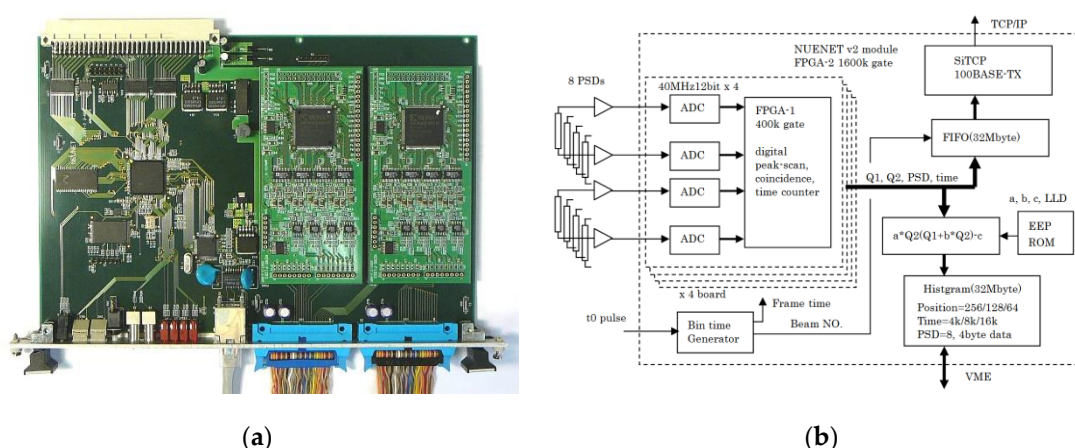
Figure 1. NeuNET: (**a**) Picture; (**b**) Block diagram. ADC: analog-to-digital converter; FPGA: field programmable gate array; PSD: linear position-sensitive ^{3}He gas detectors; TCP/IP: transmission control protocol / internet protocol; FIFO: first in first out memory; LLD: lower level discriminator; EEP ROM: electrical erasing programmable read only memory; VME: versa module Europa.

2.1.2. Scintillator Detectors

The Engineering Materials Diffractometer, TAKUMI at BL19, is one of the neutron instruments that are installed at the MLF. TAKUMI is specially designed for the analysis of residual stress and crystallographic structure of industrial materials. The commissioning of TAKUMI started in September 2008, and was completed in March 2009. The neutron detectors installed at TAKUMI [3,4] are large one-dimensional neutron detectors with a sensitive area of 1000 mm × 20 cm and a position resolution of 3 mm, as shown in Figure 2a, and have been developed under international collaboration with ISIS, Rutherford Appleton Laboratory (Didcot, UK).

The detectors were designed based on those installed in the ENGIN-X instrument of ISIS. The TAKUMI detector has 360 pixels with each size of 3 mm × 20 cm, whilst ENGIN-X detectors 240 pixels with a neutron sensitive area of 750 mm × 20 cm. TAKUMI has operated for more than 5 years with 10 detectors. In 2014–2015, 2 detectors of this type were fabricated and delivered to BL19, and thus a total of 12 detectors are now working at TAKUMI. These detectors have a neutron sensitivity of more than 50% at 1 Å and gamma-ray sensitivity of less than 10^{-6} at a gamma-ray energy of 1.3 MeV. The performance meets the requirements for residual stress analysis in neutron scattering experiments at TAKUMI.

The Single-crystal Neutron Diffractometer under Extreme Condition, SENJU, is a time-of-flight Laue single crystal diffractometer constructed at BL18. The aim of SENJU is to study crystal structures of materials under extreme environmental conditions, such as low temperature and high magnetic fields. We have developed a large-area scintillator detector using a scintillator and wavelength-shifting fiber technology [5,6]. To meet the detector specifications required for the SENJU, we designed a dedicated detector head that incorporates a 1-mm diameter wavelength-shifting fiber placed with a regular interval of 4 mm. Thicknesses of highly efficient $ZnS/^{10}B_2O_3$ scintillator screen were also optimized to ensure the detector efficiency. Figure 2b shows the developed detector module.

The detector exhibited a neutron-sensitive area of 256 × 256 mm^2, spatial resolution of 4 × 4 mm^2, and detection efficiency of 40% for 1.6-Å neutrons. The large-area detector system that includes 37 detector modules has been in service in the beamline since 2012.
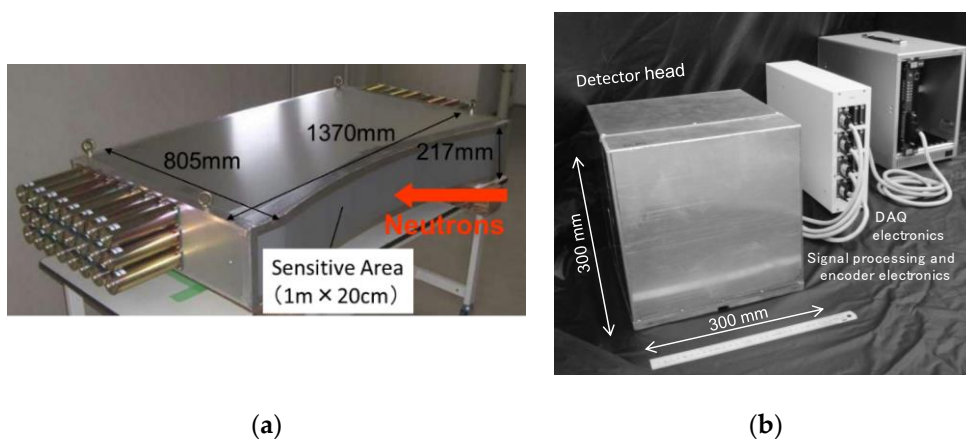
Figure 2. Photographs of (**a**) the neutron detector developed for TAKUMI and (**b**) the neutron detector developed for SENJU. DAQ: Data acquisition.

2.1.3. Gas-Based Two-Dimensional Detector

We have developed a ^{3}He gas-based two-dimensional neutron detector system for use in neutron scattering experiments using high-intensity pulsed neutrons at the Japan Proton Accelerator Research Complex (J-PARC) [7,8]. Figure 3 shows photographs of the developed detector system and of the detector head arranged in the beamline. This system exhibits superior performance, including a counting rate greater than several hundred k-cps, an average spatial resolution of less than 2.0 mm full-width at half-maximum (FWHM) with a standard deviation of 0.85 mm in the sensitive region, and a thermal neutron detection efficiency of 80%.
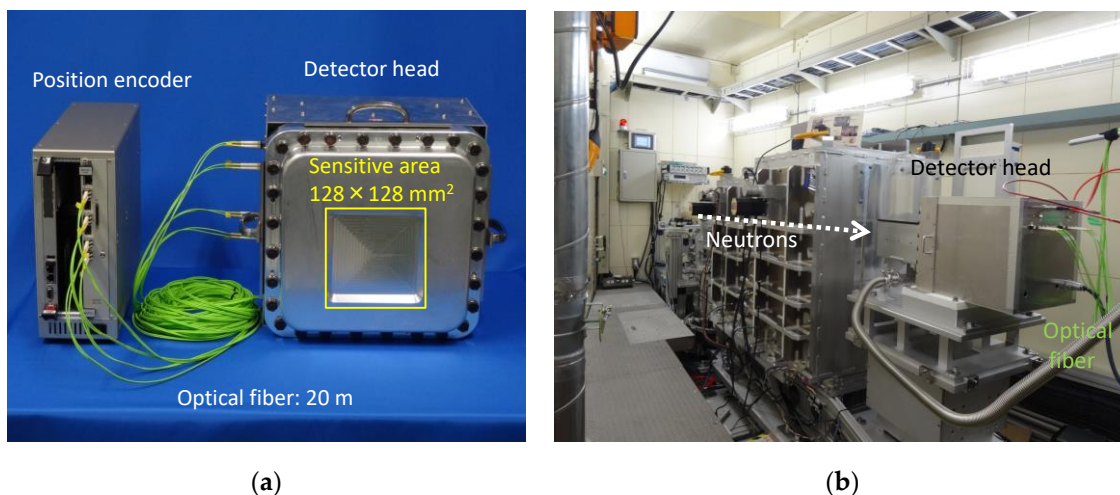

Figure 3. Photographs of (**a**) developed gas-based two-dimensional neutron detector system using individual line readout and optical signal transmission and (**b**) detector head in the beamline.

In general, a two-dimensional gaseous neutron detector has a few hundred signal lines along the vertical and horizontal axes, and the signal lines along each axis are usually connected together to conduct signal processing. The detector we have developed employs an individual line readout method, and the signal of each line is individually amplified, shaped, and discriminated by front-end electronics. A short response time and high spatial resolution can be obtained using this method. Although it is necessary to increase the gas pressure to achieve higher detection efficiency, increasing this pressure decreases the amplitude of the output neutron signal, and, consequently, discrimination between the neutron and background signals becomes difficult. Therefore, we developed a high-density

multiwire-type detector element, a low-parallax pressure vessel with multichannel feedthroughs for neutron signals, multichannel front-end electronics using dedicated integrated circuits such as application specific integrated circuits and FPGA, and optical signal transmission devices specifically for our individual-readout detector system. These dedicated devices enabled the detector system to achieve high detection efficiency, short response time, and high spatial resolution. The optical signal transmission could also be used to establish long-distance transmission between the detector head and the data acquisition device without any electrical noise.

2.2. Supermirror Devices

A supermirror [9] is composed of a total reflection mirror and sequence of multilayer monochromators whose Bragg wavelength gradually changes. The development of high-performance neutron supermirrors is important for neutron experiments since it leads to a considerable increase in the available neutron intensity at the end of the guide and beam condensers such as focusing mirrors.

A multilayer with a smaller lattice-spacing (thickness of each layer) is desirable to extend the critical angle of the supermirror, which is needed in various applications. One of the most important problems in producing a small lattice-spacing multilayer is the interface roughness, which increases with an increasing number of bilayers. If the value of the root-mean-square (rms) interface roughness can be kept small compared with the lattice-spacing, high reflectivity can be achieved by stacking a sufficient number of layers. We have developed neutron supermirrors using the ion beam sputtering (IBS) technique because it has the advantage that target atoms are sputtered with higher energy compared with the other deposition techniques. It brings good quality of layers with higher density and small grain size. In addition, the layers are not easily peeled off due to the anchoring effect [10]. In this section, we summarize the development of high-performance supermirrors and its application to MLF.

2.2.1. Fabrication and Characterization

Supermirror Coating

An IBS system with an effective deposition area of 0.2 m^2 (diameter of 500 mm) has been installed at the Japan Atomic Energy Agency (JAEA). The difference in the deposition rate has been corrected to be less than 4% over the entire deposition area by using the mask just in front of the substrate holder. The pressure before and during the process is 1×10^{-5} and 2×10^{-2} Pa, respectively.

Ni/Ti supermirrors have been fabricated with a large critical angle extended to $m = 3$, 4, and 6.7, where m is the ratio of the critical angle of the supermirror to that of Ni. Neutron reflectivities of the supermirrors at the critical angle are 0.82, 0.66, and 0.23, respectively as shown in Figure 4a [10–12] (reprinted from [10], with permission from Elsevier). NiC/Ti [13,14] supermirror with $m = 4$ was fabricated using the same IBS system. The reflectivitiy of the supermirror at the critical angle was 0.82, as shown in Figure 4b (reprinted from [14], with permission from Elsevier). The test fabrication of the NiC/Ti supermirror with $m = 6$ was performed. A reflectivity of 0.40 was realized at a momentum transfer of 1.29 nm^{-1}, corresponding to $m = 6$ [14].

Neutrons scattered from a supermirror can be divided into specular and off-specular (diffuse) components. Suppression of the diffuse component is important since it creates a serious problem of low signal-to-noise ratio when it is used in a focusing system for such purposes as a small angle scattering measurement. The diffuse intensity was decreased by more than one order of magnitude by adopting the NiC/Ti supermirror instead of the conventional Ni/Ti supermirror as shown in Figure 5 [14] (Figure 5 is reprinted from [15], with permission from American Institute of Physics). This result implies that a high-performance focusing system with a noise level down to the order of 10^{-5} compared with the focused intensity can be realized by using a NiC/Ti supermirror.
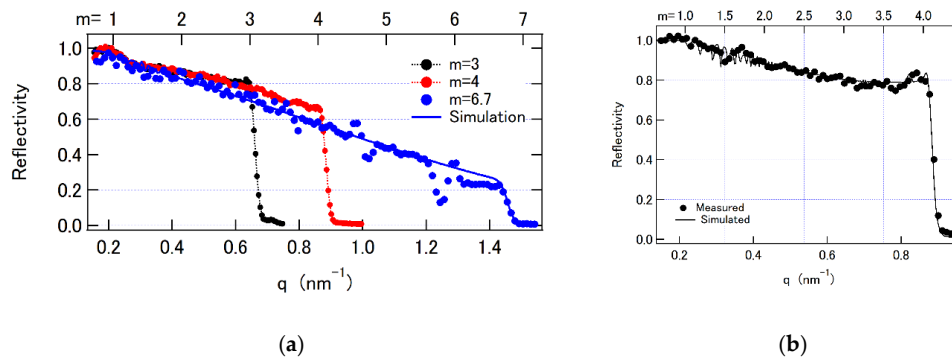
Figure 4. (**a**) Measured and simulated reflectivities of Ni/Ti supermirror with m = 3, 4, and 6.7 (8001 layers). (**b**) Measured (○) and simulated (solid line) reflectivities of NiC/Ti supermirror with m = 4. Statistical errors are less than the size of the symbols.
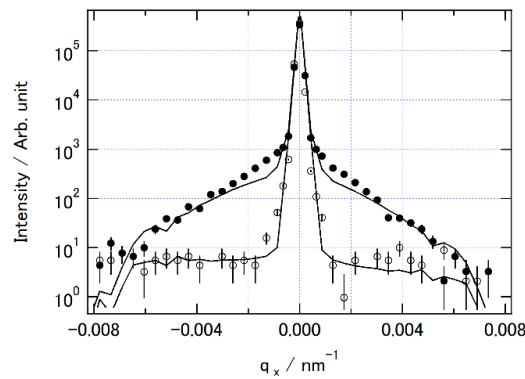

Figure 5. Measured diffuse intensity profiles of the Ni/Ti (●) and NiC/Ti (○) supermirrors (m = 3). (**a**) Rocking scan with q_z = 0.62 nm^{-1}. Solid lines indicate the calculated profiles.

Supermirror Guide

For the production of neutron guides, supermirrors were coated on float glass and borosilicate float glass substrates for the inelastic neutron scattering instruments of 4D-Space Access Neutron Spectrometer (4SEASONS) at BL01, Biomolecular Dynamics Spectrometer (DNA) at BL02, and Cold-Neutron Disk-Chopper Spectrometer (AMATERAS) at BL14 [16,17]. Figure 6 shows the guide elements produced for these instruments. The typical value of the root mean square (rms) surface roughness of the substrate was 0.3 nm and the flatness was 3×10^{-4} rad. The elliptic curve of the guide was approximately realized by the tapered guide elements. To reduce the irradiation damage due to the neutron capture reaction, the use of the borosilicate glass was avoided at the guide section close to the moderator.
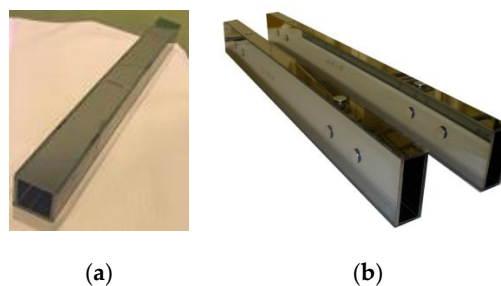

Figure 6. (**a**) A guide element at the upper stream of BL01 with a square cross-section of 90×90 mm^2. (**b**) Guide elements of BL14 with a rectangular cross-section of 90×30 mm^2.

Focusing Mirror

For spallation neutron scattering facilities, achromatic focusing optics is particularly important because most experiments are performed with wideband and focal point beams, which are indispensable for measuring micrometer-scale samples, second-resolution time-resolved measurements, or high q-resolution small angle scattering measurements. Reflective focusing mirror is a prominent candidate for that purpose. A focusing mirror needs to accept and reflect wideband beam with large divergence into a small area with high efficiency and a high signal-to-noise ratio. In order to meet these demands, we have developed ultra-precise focusing mirrors combining a high-performance neutron supermirror and a very precise surface figuring technique. A mirror substrate was prepared by figuring a surface of synthesized quartz glass into a planoelliptical shape through the Numerically Controlled Local Wet Etching (NC-LWE) process [18]. NiC/Ti supermirror (m = 4) was deposited on the quartz glass over 90×40 mm. The focal length of the ellipsoid is 1050 mm. Wideband neutrons of $\lambda > 3.64$ Å were focused with focal spot size down to 0.25 mm and peak intensity gain of up to 6 without significant diffuse scattering, as shown in Figure 7 [19]. Time-of-flight measurements suggest that wideband neutrons are effectively focused to the focal point.
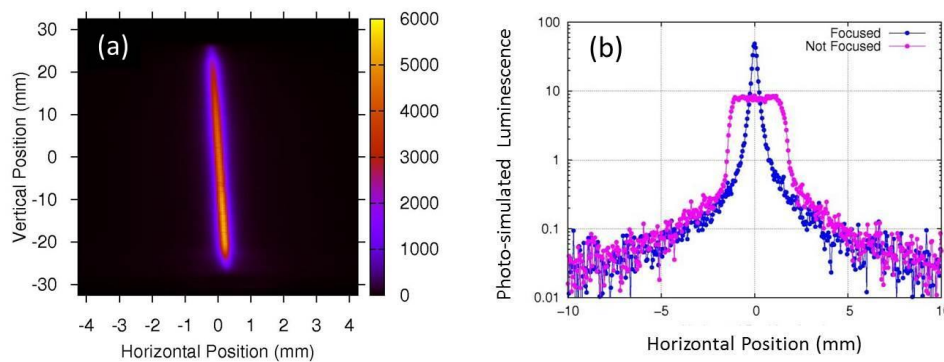

Figure 7. (**a**) Two-dimensional image of the focused beam. The tilt of the focused beam comes from the tilt of the image plate which was used in observation. (**b**) Horizontal intensity profiles of focused and unfocused beam at the vertical center.

We have developed a two-dimensional focusing device, a so-called Kirkpatrick–Baez (KB) mirror [20]. The KB mirror system is a quasi-aberration free system that consists of two total reflection elliptical mirrors placed at separate positions. One mirror with m = 4 and a length of 400 mm is used for vertical focusing and the other with m = 3 and a length of 100 mm is used for horizontal focusing. The focal length of the ellipsoid is 2100 mm. Elliptical quartz substrates were prepared by a fabrication process that combines conventional precision grinding, NC-LWE figuring and low-pressure polishing techniques. The NiC/Ti super-mirror was deposited using the IBS technique on the elliptical quartz surface. We obtained a figure error of less than 1 μm P–V (peak to valley) with a surface roughness of less than 0.3 nm rms on the supermirror. The measured focused beam width was 0.5×0.5 mm in FWHM, as shown in Figure 8.

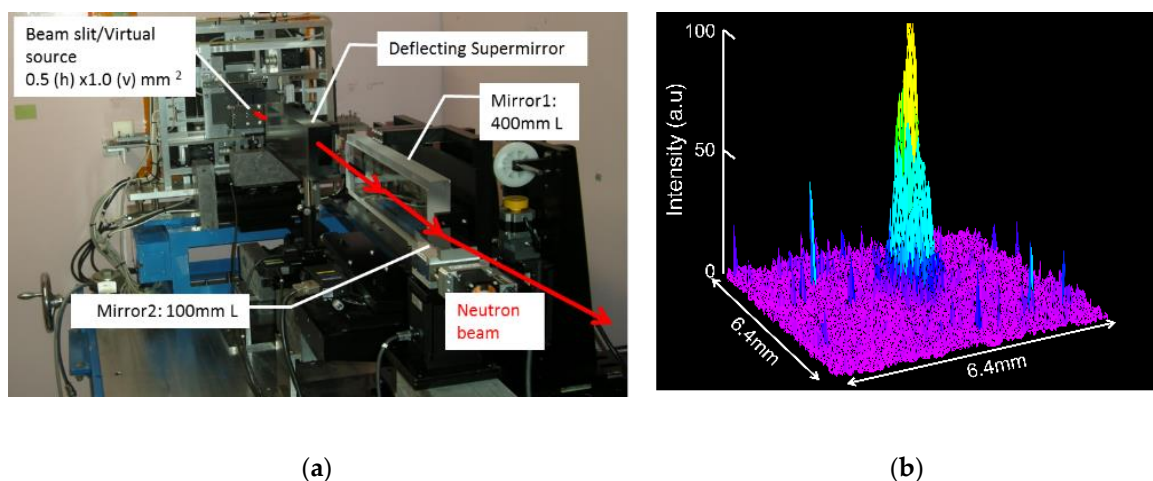(**a**)   (**b**)

Figure 8. (**a**) KB mirror configuration at NOBORU of BL10. (**b**) Focused neutron beam by the Kirkpatrick–Baez (KB) mirror has a full-width at half-maximum (FWHM) of 0.5 mm.

2.3. ^{3}He Neutron Spin Filters

In order to apply a ^{3}He neutron spin filter (NSF) to experiments at a pulsed neutron experimental facility, it is important to make the setup stable and easy to set up and operate, because the setup is located inside a radiation shield for high-energy gamma rays and neutrons. Moreover, a uniform magnetic field is essential to achieve a very high nuclear polarization. In this study, we have developed compact laser optics with a volume holographic grating (VHG) element and a flexible non-magnetic heater with a thickness of less than a half millimeter and a thermal tolerance up to 300 °C for a spin-exchange optical pumping (SEOP) method, and composed a setup for an in situ SEOP ^{3}He NSF. The design and performance of the setup will be described in the following sections.

2.3.1. Compact Laser Optics

We have developed compact laser optics with an air-cooled laser diode array (LDA) which does not need a water chiller to operate it. As the output laser power of the air-cooled LDA, which is around 30–40 W, is much lower than that of a water-cooled one, is enough to polarize ^{3}He gas within a small-sized cell [21]. The laser spectrum of the LDA is broader than the absorption line width of Rb [22]. Thus, we employed a VHG element to create an external cavity laser (ECL) to narrow the width of the laser spectrum to match it to the absorption line width of Rb [23] (Figure 9). The developed laser optics are shown in Figure 9. The LDA is cooled with a Peltier device and a fan. The temperature of the VHG is controlled within ±1 °C using a heater. Collimating and shaping lenses and a λ/4 wave plate were assembled in a box (Figure 9). Therefore, the circularly polarized laser, which is necessary for the SEOP [21], is extracted from the box.

The measured laser spectra with and without the feedback are shown in Figure 10. The laser spectrum was narrowed to be a FWHM of 0.35 nm by the feedback, which is 16% of the original spectrum width without the feedback (Figure 10). The specification value of the spectrum width of the VHG element is 0.14 nm. The observed spectrum width obtained with the feedback was about 2.5 times that of the specification value of the VHG. This may be due to a miss-alignment of the optical components such as the so-called *smile* of the LDA (The *smile* is defined as the bending of the line of emitters of the LDA [24,25]). Here, the value of the *smile* of the LDA was unknown and was not also guaranteed by the supplier. To check for the *smile* effect, we tentatively set up the optics with the same geometry with a LDA which had the lower *smile* of less than 1 μm, and evaluated the laser spectrum. The obtained spectrum width was a FWHM of 0.18 nm (Figure 10), which was closer to the specification value of the VHG.
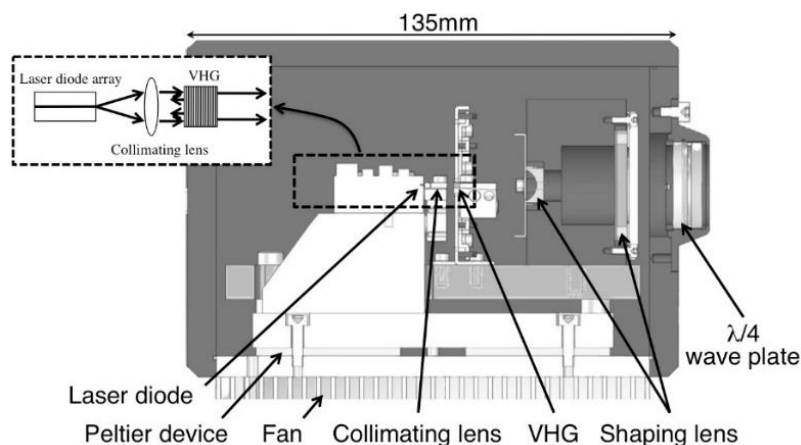
Figure 9. A drawing of the developed laser optics. The inset shows the schematic layout of the external cavity. VHG: volume holographic grating.
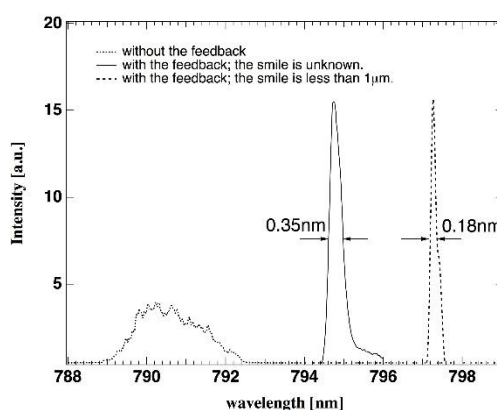

Figure 10. The measured laser spectra with and without the feedback to narrow the spectrum.

Then we assembled a setup for the in situ SEOP ^{3}He NSF with the developed laser optics, and applied it the neutron beam experiments at the polarized neutron reflectometer, SHARAKU (BL17) [26], and the small-angle neutron scattering instrument, TAIKAN (BL15) [27], at MLF, where an ^{3}He polarization degree of 0.68 was achieved and maintained during the experiments [26,27].

2.3.2. A Non-Magnetic Flexible Heater

In SEOP [28], the number density of alkali metal vapor is one of the important parameters to efficiently polarize ^{3}He nuclei. The appropriate number density is on the order of $10^{15}/\mathrm{cm}^3$ and the corresponding temperature is between 160 °C and 250 °C depending on the K and Rb mixture in alkali-hybrid SEOP [29]. Hot air blowers, which introduce no magnetic fields to the ^{3}He cells, are commonly used to keep ^{3}He cells at appropriate temperatures since ^{3}He nuclei are extremely sensitive to magnetic field gradients and the polarization can easily be lost to unwanted stray fields. Instead of hot air blowers, electrical heaters are occasionally used with extreme caution not to interfere the magnetic field at the cell position [30,31]. Using such an electrical heater allows one to reduce the size of a neutron spin filter as well as enhance safety compared to the use of a hot air blower.

Our non-magnetic flexible heater has two heating layers made of Ni–Cr foil with specially designed strip patterns. The two heating layers are separated and covered by polyimide film for electrical insulation, as illustrated in Figure 11. The two layers of the Ni–Cr foil have an identical strip pattern, and the electrical current through each strip is in the opposite direction so that the magnetic fields produced by the heater currents cancel each other.

Figure 11. The structure of non-magnetic flexible heater. Two layers of Ni–Cr foil are sandwiched between a polyimide film for electrical insulation. The overall thickness of the heater is less than 0.5 mm.

The non-magnetic flexible heater is wrapped on a cylindrical aluminum oven with a diameter of 120 mm and a length of 150 mm to heat a ^{3}He cell inside it (Figure 12).
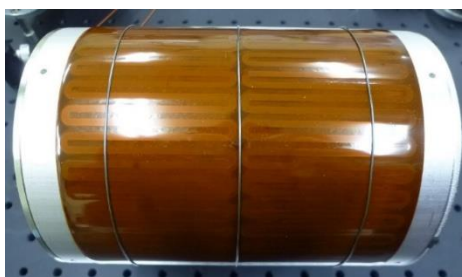

Figure 12. The non-magnetic flexible heater on a cylindrical aluminum oven. The heater is tightened with non-magnetic brass wires. Additional polyimide foam insulator, which is removed for the picture, covers the heater.

The performance of the non-magnetic flexible heater was measured using a polarized ^{3}He cell placed inside the aluminum oven with the heater current on. Figure 13 shows the spin-relaxation rate measured for a ^{3}He cell to different electrical currents, and it was found that there were no influences on the ^{3}He spin relaxation by the heater current. Note that the operating heater current is less than 1 A for the actual alkali-hybrid SEOP.

We have successfully developed a non-magnetic flexible heater with an excellent performance for the SEOP applications [32]. Such non-magnetic flexible heaters can also be used in other applications that require no magnetic interferences.
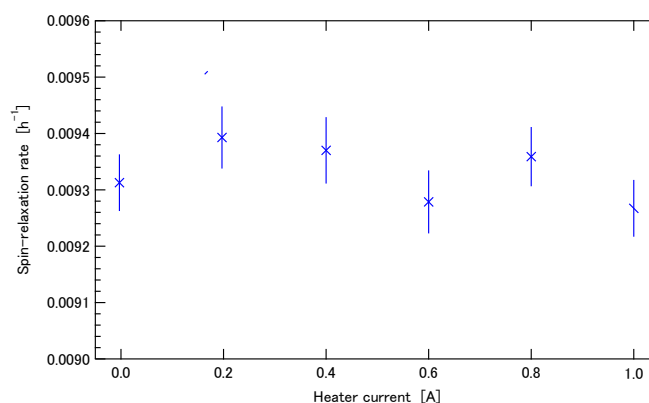

Figure 13. The spin-relaxation time of a ^{3}He cell was measured to the heater current. No current dependence was observed.

2.4. Choppers

2.4.1. T0 Choppers

A T0 chopper is equipped with a massive blade to reduce background noise originating from the high-energy neutron burst. To utilize eV neutrons, we developed a T0 chopper rotating up to 100 Hz [33]. On the high-resolution chopper spectrometer (HRC) at BL12, the dimension of the chopper blade (shielding part) on the rotor is $78 \times 78 \times 300$ mm (300 mm is the length along the neutron beam) with a margin of $\Delta w = \pm 1$ mm (the beam cross section is 76×76 mm). This margin corresponds to the phase control accuracy of $\Delta t = \pm 5$ μs at $f = 100$ Hz ($\Delta t = \Delta w/2\pi Rf$), for the rotational radius $R = 300$ mm. Since this T0 chopper is installed 9 m from the neutron source, neutrons with energies up to 2.5 eV can be utilized. In this T0 chopper, the rotor made of Inconel X 750 is mounted inside the vacuum, the shaft is supported by ball bearings, and the rotation is transferred through a magnetic seal from the motor located outside the vacuum chamber, as shown in Figure 14a. The length of the T0 chopper along the neutron beam is 1.3 m. A continuous running time of more than 1000 h and a total running time of more than 4000 h are required without changing components, and we confirmed these requirements. The maintenance should be scheduled considering these periods. The performance of the T0 chopper on HRC is indicated in Figure 14b. A neutron beam monochromatized by a Fermi chopper rotating at 600 Hz is incident upon a vanadium (V) sample and scattering neutrons are measured as a function of TOF. The peaks at around 1940, 4200, and 6460 μs, which correspond to 502, 108, and 45 meV, respectively, are of properly monochromatized neutrons (the peaks at 810 and 3070 μs are from half-turns of the rotation). The background noise is successfully reduced by 2 orders of magnitude at around 500 meV. A variety of requirements from instruments can be covered by a small modification of the structure: a short model less than 1 m long with $f = 50$ Hz for the total scattering instrument NOVA at BL21, and a two-beamhole model with $f = 25$ Hz for the reflectometer SOFIA at BL16. Also, this type of T0 chopper is used in BL04, BL22, and BL23.

(a)   (b)
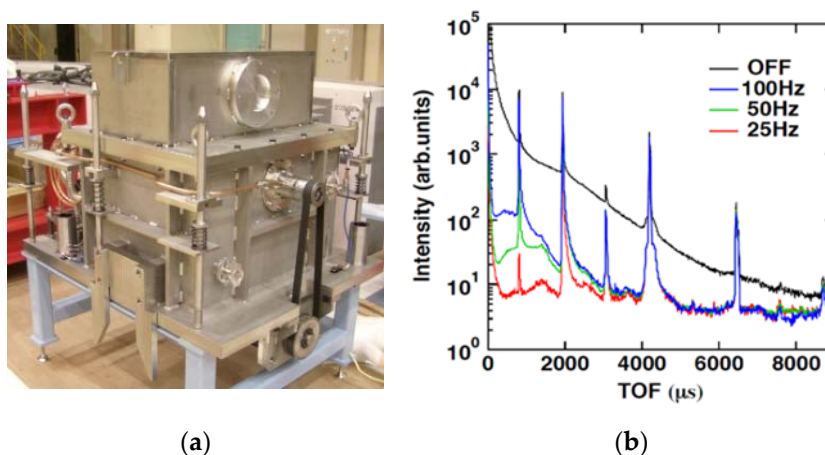
Figure 14. (**a**) Photograph of the T0 chopper installed on high resolution chopper spectrometer HRC. (**b**) Effect of background noise reduction. Time-of-flight (TOF) spectra for the operation at $f = 100$ Hz, 50 Hz, 25 Hz, and in no operation (OFF) condition are indicated.

Another type of T0 chopper is also being used at MLF. The development target for this T0 chopper was to make the length along the beam path as short as possible, which enables us to minimize the loss of neutron transport. To make our target a success we introduce an in-wheel type motor to the T0 chopper. This motor has an inner stationary portion (the stator), and an outer rotating portion (the outer rotor) that rotates around the stator and drives a chopper blade (Inconel X 750) attached to the outer rotor.

Many years of research and development in collaboration with Kobe Steel Co., Ltd., (Kobe, Japan) (KOBELCO) have accomplished the compact type T0 chopper system [34]. The dimension of the T0 chopper blade for BL01 is 84 mm (cross section) × 300 mm (length along the beam). Each beamline (BL) has a different cross section, determined by the beam size at the location of a T0 chopper. The first product of a compact type T0 chopper is shown in Figure 15a. The length along the beam path is reduced to 500 mm, and the upper limit of rotating frequency is 50 Hz. The inelastic neutron scattering data measured on 4SEASONS at BL01 with and without a compact type T0 chopper are shown in Figure 15b,c, respectively. The background in the high-energy region is significantly suppressed [35]. The compact type T0 chopper is used at BL01, BL09, BL11, BL15, BL18, and BL20. We are now working on research and development of the compact type T0 chopper, aiming at increasing the upper limit of the rotating frequency, which further extends the usable incident energies toward the higher energy side.
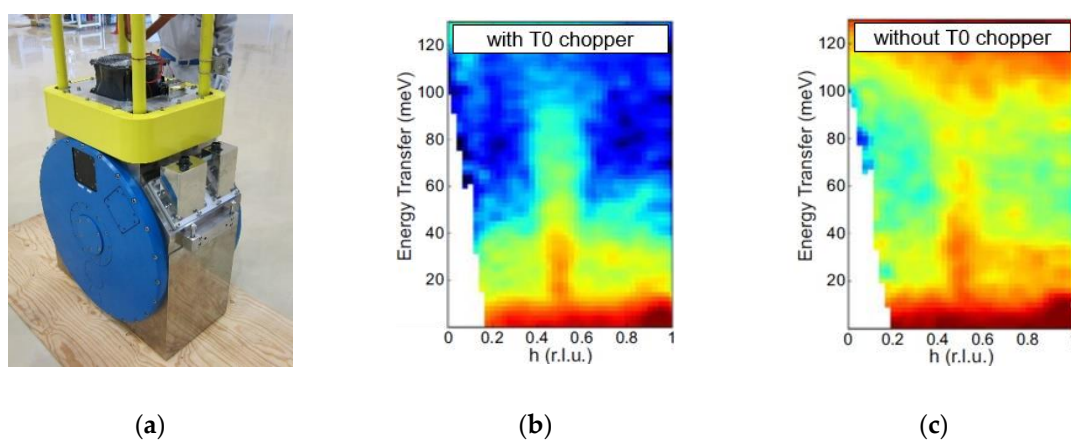

(**a**)   (**b**)   (**c**)

Figure 15. (**a**) Photograph of the compact type T0 chopper for 4SEASONS. Inelastic neutron scattering data obtained by 4SEASONS (**b**) with and (**c**) without the compact type T0 chopper.

2.4.2. Fermi Choppers

A Fermi chopper consists of a rotating slit package to monochromatize neutron beam [36]. We developed a Fermi chopper (Figure 16a) [37] by using a magnetic bearing mounted in a turbo molecular pump whose pumping speed is 1300 L/s, because the mass and the moment of inertia of its rotor blade are almost identical to those of the slit package of the Fermi chopper. This system can be operated in a range of rotational frequencies (f = 100–600 Hz). On HRC, the energy resolution with respect to the incident neutron energy is $\Delta E/E_i$ = 2.5% for the optimum condition $\Delta t_{ch} = \Delta t_m$, where Δt_{ch} is the chopper open time and Δt_m is the pulse width, and, further, $\Delta E/E_i$ = 1% is achieved if Δt_{ch} = 1 μs is realized for eV neutrons. The phase control accuracy Δt should be less than 30% of Δt_{ch} to minimize intensity loss. We assumed that $\Delta t \leq 0.3$ μs, i.e., a frequency resolution $\Delta f = |df/dt| \Delta t = f^2 \Delta t \leq 0.01$ Hz at f = 600 Hz, as the goal of the development. The phase control system was developed using a direct digital synthesizer system with a frequency control unit of 0.00058 Hz at f = 600 Hz. The phase control accuracy in the developed Fermi chopper was observed to be Δt = 0.08 μs at f = 600 Hz, well within the specification of the goal. An inelastic neutron spectrum from a vanadium sample measured by using this Fermi chopper on HRC is shown in Figure 16b, where the energy resolution for E_i = 206 meV is identical to the designed standard resolution of $\Delta E/E_i$ = 2.5%. This type of Fermi chopper is also used on BL21 and BL23.

Furthermore, we have proposed a new method of inelastic neutron scattering measurement in chopper spectrometer by simultaneously utilizing the multiple incident energies (E_i) [38]. This method (Multi-E_i measurement) can reduce the dead time in time-of-flight measurement, and thus can markedly increase the measurement efficiency. Generally, a Fermi chopper is not suitable for Multi-E_i

measurement, because transmission of a Fermi chopper is usually optimized to a specific E_i by curved slits. On 4SEASONS, however, we decided to adopt a Fermi chopper with straight slits that sacrifices the transmitted intensity but passes through a wide energy range of E_i. This decision brought us success in the experimental demonstration of the usefulness of Multi-E_i measurement, even in the Fermi chopper spectrometer [39].
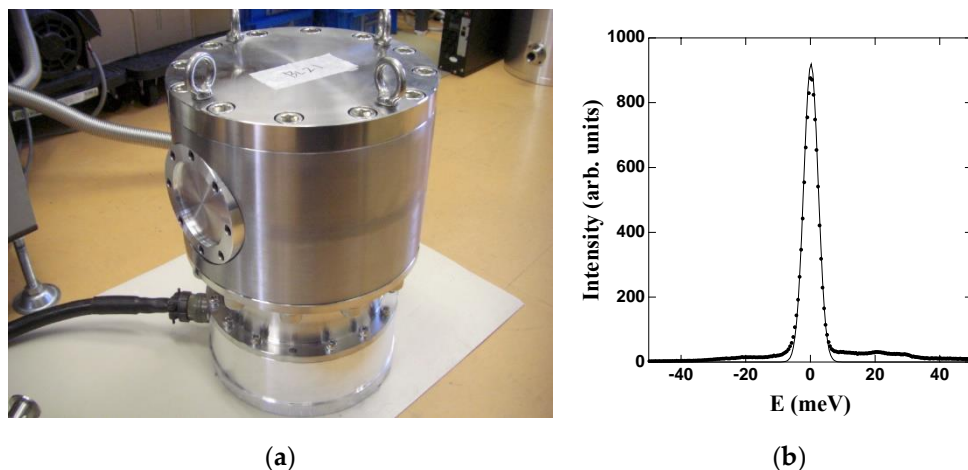
Figure 16. (**a**) Photograph of Fermi chopper. (**b**) Observed inelastic scattering spectrum from a vanadium sample for E_i = 206 meV with the Fermi chopper rotating at f = 600 Hz on HRC. The FWHM of the peak is ΔE = 5.4 meV.

We have continuously re-examined the performance of the Fermi chopper. Recently, we replaced the existing Fermi chopper of 4SEASONS with a newly developed one that has a more compact slit package [40]. The new Fermi chopper provides us with more neutron flux without lowering the resolution. The inelastic neutron scattering data of vitreous silica, measured at 4SEASONS using the previous Fermi chopper and the new one, are compared in Figure 17. The measurement time was 30 min for both.

Figure 17. *Cont.*

(**c**)

Figure 17. Inelastic neutron scattering spectra of vitreous silica measured at 4SEASONS by using (**a**) the previous Fermi chopp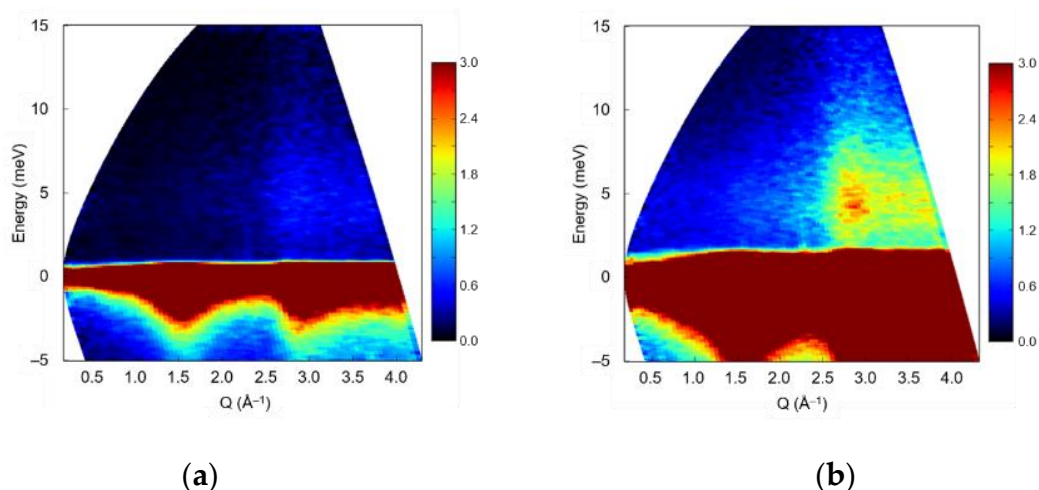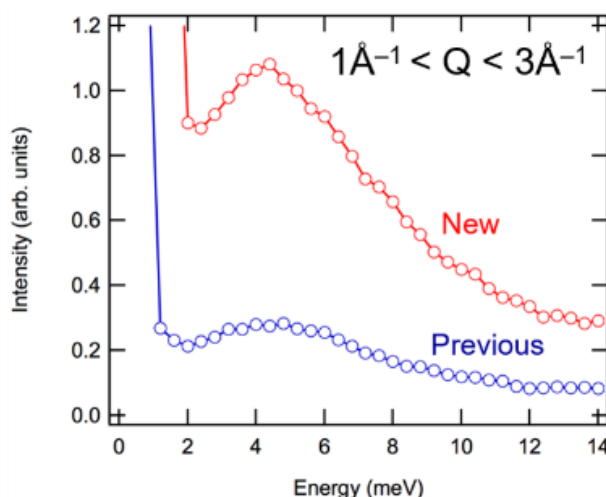er and (**b**) the new one. The measurement time was 30 min for both. (**c**) A comparison of the energy dependences of *S(Q, E)* between the previous Fermi chopper and the new one.

2.4.3. Disk Choppers

Neutron disk-choppers are simple but indispensable devices for neutron spectrometers. Therefore, most of the neutron instruments at MLF employ disk-choppers. The disk-choppers employed at constructed and planned neutron instruments at MLF are listed in Table 1. At MLF, two types of disk-choppers are used. One is a slow disk-chopper, which runs at a relatively slow speed, $f \leq 50$ Hz, and is used to define the band width or frame and eliminate undesired neutrons. The other one is a fast disk-chopper, the maximum revolution of which can exceed 300 Hz, and is used in a monochromator or for shaping the pulse width of the neutron beam coming from source. Pulse shaping is a rather special task of the fast disk-choppers at MLF, since some inelastic instruments utilize high intensity from the coupled moderator source by shaping a broad pulse shape from this type of source by fast disk-choppers to realize high intensity and high resolution simultaneously. Therefore, as much effort has been devoted to fast disk-choppers as to slow disk-choppers.

Two main benders, KOBELCO and MEISYO KIKO, provide disk-choppers to the instruments at MLF. There we try to unify the menu terms, look, and feel so as not to confuse the two.

Commissioning of disk-choppers was conducted by an MLF chopper task team. The electronic noise level, which can affect other devices in the experimental halls, and performance (phase stability, transmission of the disks, temperature evolution of spindles and housing, etc.) were investigated for all disk-choppers installed in instruments at MLF. The information is shared by all instrumental teams through this task team.

Slow Disk-Choppers

The slow-speed disk chopper was developed for the device as a band definition chopper or a frame-overlap suppression chopper or a pulse suppression chopper, for example at 12.5 Hz.

The prototype slow disk chopper was developed from 2004 with KOBELCO. Its main specifications are as follows.

(i)　For the ease of maintenance, the neutron beam is passed under part of the disk chopper, and the body of chopper disk and motor are mounted on the stand (see Figure 18).

(ii)   For the reduction of disk weight, the disk was made of an Al alloy applied with (isotope enriched $^{10}B_4C$ powder + epoxy resin) as a neutron absorber.

(iii)   The transmission of neutrons was less than 10^{-6} at E_i = 100 meV.

Nowadays many slow disk choppers are produced and installed in many beamlines, which are designed referring to the prototype slow disk chopper, even in those produced by MEISYO (see Table 1). On the slow single disk chopper installed in BL19, we performed some commissioning tests. Figure 19 shows the commissioning results. From this phase control test, we determined the operational parameter for this disk chopper.

Table 1. Disk Choppers at the Materials Life Science Facility (MLF).

Beam Line	Type of Chopper (No.)	Manufacturers
BL01	SI(2)	KOBELCO
BL02	FII(1), FI(2), SII(2), SI(1)	KOBELCO
BL03	SI(1)	MEISYO
BL04	SII(1)	MEISYO
BL05	none	-
BL06	SI(2)	Vacuum Products.
BL08	SII(1), SI(2)	MEISYO
BL09	SI(3)	MEISYO
BL10	SI(1)	MEISYO
BL11	SI(2)	KOBELCO
BL12	none	-
BL14	FII(2), FI(2), SII(2)	KOBELCO
BL15	SI(3)	KOBELCO
BL16	SI(1)	Vacuum Products.
BL17	SI(3)	KOBELCO
BL18	SI(2)	KOBELCO
BL19	SI(1)	KOBELCO
BL20	SII(1), SI(2)	MEISYO
BL21	SI(1)	MEISYO
BL22	SII(1)	MEISYO
BL23	FI(1) correlation, SI(2)	MEISYO

S: slow chopper; F: fast chopper; I: single disk; II: double disk (number of that type chopper in the beamline).
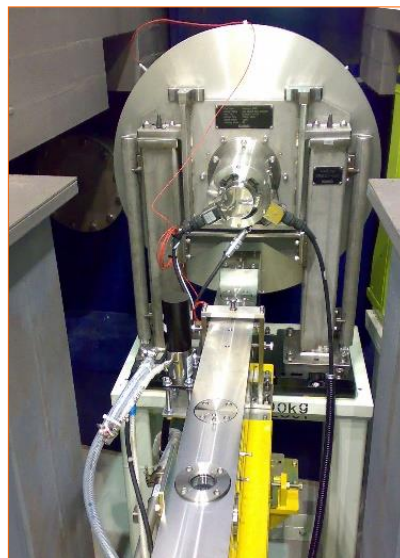

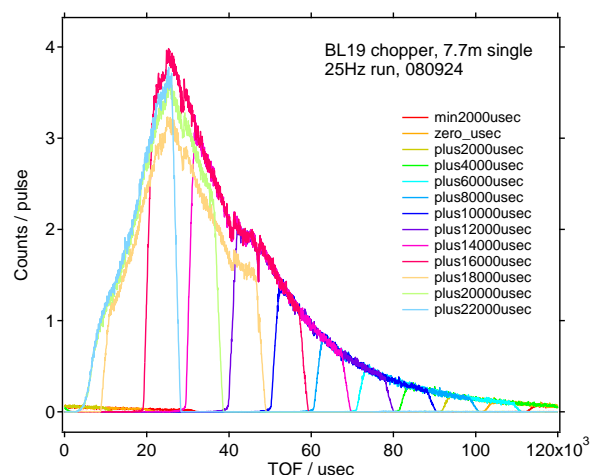**Figure 18.** The slow single disk chopper installed in BL19.

Figure 19. Phase control test on the slow single chopper in BL19. It shows the incident beam TOF spectrum selected by the disk chopper in several phase delay conditions.

Fast Disk-Choppers

The development of fast disk-choppers started in 2004 with KOBELCO. The cold-neutron disk-chopper spectrometer AMATERAS (BL14) requires a minimum burst time of less than 8 μs to realize 1% energy resolution. The requirement was that a disk of 600 mm diameter with a 1 cm slit should run at 350 Hz revolution. In 2004, such disk-choppers were not available, which is why we started developing them. There were several technical issues during the development. The most important key is the disk itself. After experiencing several crashes of disks and sometimes even a full chopper system, finally disks can be run at a revolution of >350Hz (Figure 20a). Special care was taken in optimizing the direction of carbon fibers of carbon fiber reinforced plastic (CFRP) and the method of placing. Also, we used the metal ^{10}B, not ^{10}B$_4$C, to reduce the mass at the edge of the disk.

(**a**)   (**b**)
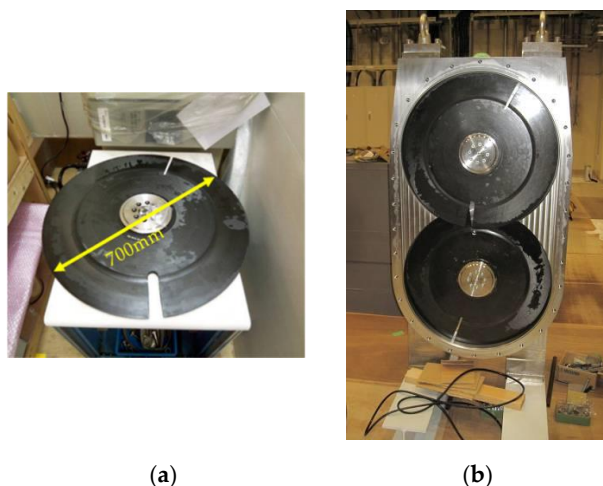
Figure 20. (**a**) A disk for fast-disk choppers and (**b**) inside view of No. 2 fast-disk chopper of AMATERAS.

At MLF, three sets of fast disk-choppers have been installed at AMATERAS. Specifications of the three choppers of AMATERAS are listed in Table 2. No. 1 chopper shapes the width of a pulse from the source. No. 2 chopper is the monochromator chopper. No. 3 chopper is used for removing unwanted neutrons coming through No. 1 choppers. Motors and disks of No. 2 chopper are placed one above the other to set two disks as close together as possible (Figure 20b).

This is essential to perform multi-E_i measurements on AMATERAS [38]. Commissioning of fast disk-choppers has been done in the course of the commissioning of AMATERAS. By using these choppers, we have confirmed $\Delta E/E_i \sim 1\%$ energy resolution in the range of $E_i \leq 3$ meV.

Based on the experience of developing fast disk-choppers of AMATERAS, in 2011 we manufactured other fast disk-choppers for the biomolecular dynamics spectrometer DNA (BL02). DNA uses three sets of fast disk-choppers (one of 225 Hz—double-disk type with 4 slits (1 cm × 1 slit and 3 cm × 3 slits) for pulse shaping and two of 150 Hz—single-disk type with 4 and 2 wide slits, respectively, for removing unwanted neutrons); these choppers have been working since 2012.

Table 2. Fast disk-choppers installed at AMATERAS and DNA.

AMATERAS	No. 1	No. 2	No. 3
$L_\text{modrator-chopper}$	7.1 m	28.4 m	14.2 m
Disk Radius	350 mm	350 mm	350 mm
Revolution	≤350 Hz	≤350 Hz	≤350 Hz
No. of Disks	2 (Counter-Rotating)	2 (Counter-Rotating)	1
Slit Width	30 mm	10 & 30 mm	30 mm
Min. Burst Time	22.7 μs	7.6 μs	45.5 μs
Gap between Disks	50 mm	20 mm	-
DNA	**No. 1**	**No. 2**	**No. 3**
$L_\text{modrator-chopper}$	7.750 m	11.625 m	23.250 m
Disk Radius	350 mm	350 mm	350 mm
Revolution	≤225 Hz	≤150 Hz	≤150 Hz
No. of Disks	2 (Counter-Rotating)	1	1
Slit Width (deg.)	1.9 (10mm) & 5.7 (30 mm)	24.7	56.6
No. of Slits Min. Burst	4	4	2
Time	12 μs & 36 μs	-	-
Gap between Disks	50 mm	-	-

3. Computational Environment

Software now plays an indispensable role in scientific research in all fields. In neutron and muon measurement, software affects the efficiencies of all processes such as planning of measurements, optimization of hardware condition, hardware control, collection of data, data correction of hardware dependent factors, model constructions, comparison with theories, and so on.

The MLF computational environment was started in 2003. Five software components were defined: experiment, analysis, simulation, database components, and a user interface to integrate these components. Under a collaboration with KEK Computing Research Center (Tsukuba, Japan) a prototype of the data analysis framework with C++ was built in 2004 as the core of the analysis component [41]. It was four years before the operation of MLF. Until day 1 of MLF in 2008, two components were developed: (1) core of the experiment component, DAQ-Middleware for MLF neutron scattering [42], in the collaboration with the Particle and Nuclear Laboratory, KEK; and (2) a user interface component (IROHA). The network infrastructure of MLF was established by the J-PARC information section. Since then, each component has been developed.

International collaboration has been pursued with ISIS facility, Rutherford Appleton Laboratory and Spallation Neutron Source (SNS), Oak Ridge National Laboratory (Oak Ridge, TN, USA) [43]. Unfortunately, the collaboration is not successful so far since the software development was insufficient at MLF then. However, to catch up with the very rapid progress of software, international collaboration is still desired.

In this section, the described MLF computational environment focused on the neutron scattering facility. The computational environment of the Muon facility is different but some of

the components, such as the user interface (IROHA2, described in Section IROHA2), will be used as common components.

3.1. Main Components of MLF Computational Environment

3.1.1. Instrument Control Software Framework: IROHA

Overview of Instrument Control Software

The software for instrument control should be user-friendly, scalable, and flexible for MLF experiments. To satisfy these requirements, we have developed a common software framework, called IROHA, for instrument control at MLF [44,45]. The characteristics of IROHA are as follows:

- Scalability: high throughput for large-scale data on the gigabyte order.
- Flexibility: adaptability of various experimental purposes by providing hardware control software for a variety of hardware.
- User-friendly: graphical user interface and controllable via remote access.
- Automation: programing measurement with graphical user interface as well as command-line interface.

IROHA

During the construction period of MLF, we have developed an instrument control software, IROHA, which consists of the common graphical user interface (GUI) software called Working Desktop (WD) and experimental controlling software to operate DAQ hardware and other equipment such as SE equipment and beamline optics components. The source code of IROHA was written in an object-orientated script language, Python, and XML/HTTP was chosen as the protocol between software components. Users can perform their experiments and data analysis by sending Python commands through IROHA. In other words, users can seamlessly operate experimental controlling, data analysis, and visualization with one Python script. IROHA is introduced to the many instruments of MLF and currently used in MLF users' experiments.

IROHA2

Several years ago, we started to upgrade IROHA to improve the following points [46,47]:

1. Proper role-sharing between the software of individual device control and that of the integrated instrument control.
2. The interface with database systems such as MLF experimental database (MLF EXP-DB), the authentication system, the user information database cooperated with the system of J-PARC Users' office for linking metadata with experimental data.
3. Platform-independent user interface.

The new software framework for instrument control at MLF, named IROHA2, was first released in 2013 and introduced to several instruments and users' experiments.

For proper role-sharing of software, IROHA2 consists of four software components:

- Device control server: operation, monitoring and logging outputs of devices. More than 50 devices have been supported.
- Instrument management server: generation of run information, configuration and management of instrument components and user authentication.
- Sequence management server: configuration and management of automatic measurement.
- Integrate control server: integral operation and monitoring of an instrument; monitoring is also available from outside of MLF.

The interfaces with database systems in IROHA2 are the main function of the instrument management server. The instrument management server generates run information included the URI (Uniform Resource Identifier) of the measurement data (from the DAQ system), the user ID, the title of the experiment, the sample information (from the user information database), device information (from the device control servers), and the measurement time of each measurement. Because run information is written in XML format, we can describe various data flexibly. MLF EXP-DB collects and catalogs the run information for the management of experimental data.

We have introduced a web interface as a platform-independent user interface for IROHA2. Users can access IROHA2 not only from desktop computers but also from mobile devices such as tablets and smartphones with a web browser on each operating system. More than 50 devices have been supported by the device control server of IROHA2.

Issues with IROHA2 are follows: (1) supporting more devices, especially users' devices brought to MLF; (2) introduction of a real-time communication method such as a message queue, instead of recording data files, for 1 MW operation; (3) continuous improvements towards a user-friendly interface.

3.1.2. Data Acquisition

Event Recording Method

The standard DAQ mode at MLF is the event recording method [48,49]. The event recording method has realized that each signal that is a detection of neutrons and muons, conditions of SE equipment (position of stage, angle of goniometer, temperature, pressure, magnetic and electric field, etc.), status of beamline optical components (injection beam intensity, slit size, phase delay of chopper, neutron polarization, etc.), timing of proton injections, and so on, is recorded as an event with the timestamp. We have assembled the event recording system for these various events as shown in Figure 21. Many kinds of signals are input to the DAQ boards (GateNET, TrigNET, NeuNET, and Readout) and converted into event data. The event data are collected and stored by the DAQ-Middleware running in DAQ computers.
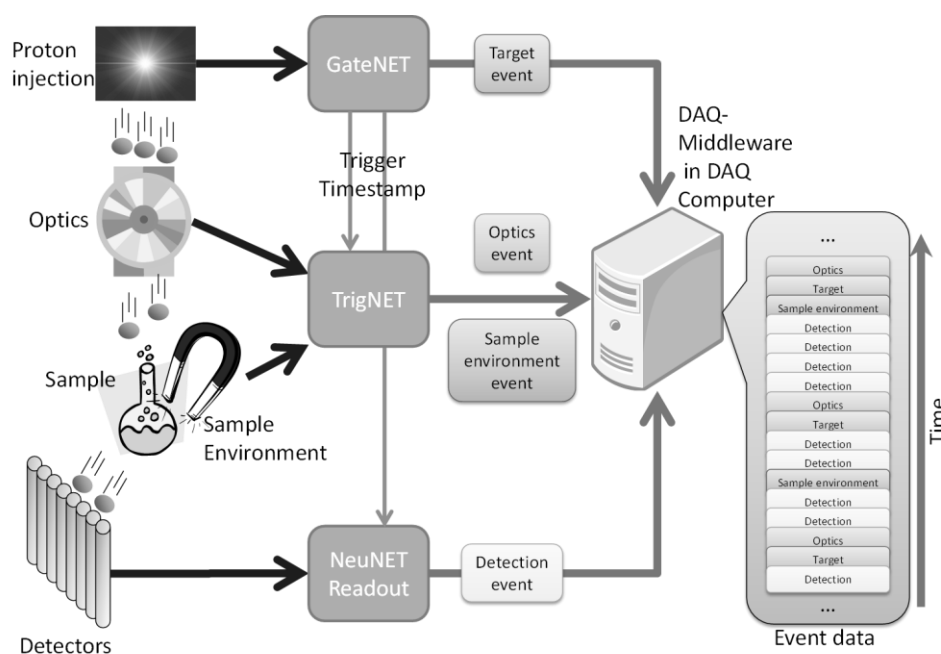

Figure 21. Diagram of event recording method.

High-throughput performance is necessary in the event recording method in a high-intensity facility like MLF. We have realized this by introducing a distributed network environment into the DAQ boards and software. The boards have incorporated a SiTCP Ethernet interface [50], which is fieldbus network protocol technology. The DAQ software incorporated DAQ-Middleware, which is easily configurable DAQ software under a distributed network environment.

The event recording method realized data reduction of neutron scattering combined with every recorded events. This is described in the data reduction section.

Data Acquisition Software

DAQ-Middleware [51–53] is a data acquisition software framework developed at KEK. We can build the DAQ software by assembling several DAQ components of DAQ-Middleware in flexible and scalable. In addition, DAQ-Middleware can make the DAQ component include customized logic. Because these characteristics satisfy our demands, we have adopted DAQ-Middleware as the standard DAQ software at MLF, installed on all the DAQ computers of the many MLF instruments. We have developed various readout components according to detectors equipped in MLF instruments and the components to produce data for monitoring and analysis.

3.1.3. Data Reduction and Visualization

Overview

In general, there are many procedures for data analysis to obtain scientific results from measured data. The MLF computational environment group clearly separates these procedures into two parts, as below.

1. Data Reduction

    -   Conversion from the binary raw data, i.e., the event recording data at MLF, to the histograms format.
    -   Data correction, for example the detector efficiency, the solid angle, the background subtraction, the calculation of absolute value on the structure factor, and so on.

2. Data Analysis

    -   Interpretation of measured data, like structure refinement and simulation calculation.

Our group mainly produced the data reduction software by ourselves because we regard it as a part of hardware of instruments. It is expected that a deep commitment to data reduction will make it possible to quickly catch up with advanced hardware technologies and to develop novel measurement and analysis methods for MLF users. For data analysis, on the other hand, we decided that users should utilize not only our software but also external popular software because the analysis software is strongly dependent on a user's particular type of science and we have poor development resources. We, therefore, offer some conversion software from our data format to that of external software. In addition, we also produced the basic visualization software ourselves, while the advanced visualizations are treated as a part of the data analysis.

We developed framework software for data reduction and analysis to unify data formats and functions at the MLF facility at first. Next, we developed some of the data reduction and visualization software on this framework. These results are mentioned in the following sections.

Object-Oriented Data Reduction and Analysis Framework Manyo Library

Many neutron scattering instruments have been installed at MLF, but requirements of data reduction and analysis software for each instrument are quite different among instruments. The MLF computational group has developed a software framework for developing data reduction and analysis

software that can be applied to each type of instrument [41,54,55]. Now the framework Manyo Library is working on the 16 instruments that are shown in Figure 22. The framework provides fundamental and generic functionalities for developing application software for neutron scattering experiments. Because three-dimensional histograms should be handled in the framework, we developed a series of data containers that can be applied to one-, two-, and three-dimensional histograms. ElementContainer (EC) is a simple and fundamental data container in the framework, which can store a one-dimensional histogram with its error values, where any number of vector objects can be kept with their names and metadata. Users can access each data object with its name. Data containers for two- and three-dimensional histograms, ElementContainerArray (ECA) and ElementContainerMatrix (ECM), are also prepared (Figure 23). One-, two-, and three-dimensional histogram data are stored in the EC family with their metadata, and four arithmetic operations between them can be performed with error propagations.
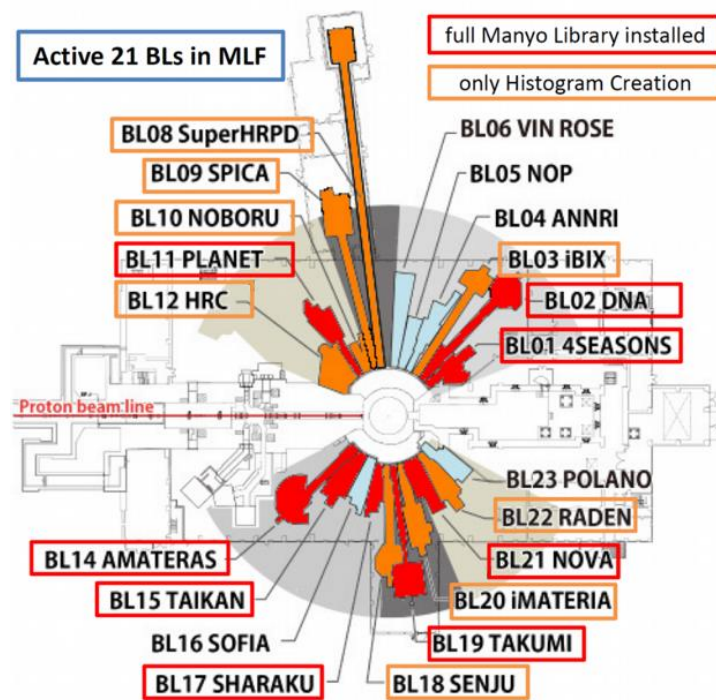

Figure 22. Floor layout of MLF. The Manyo Library is working on the 16 beamlines indicated by orange and red boxes.
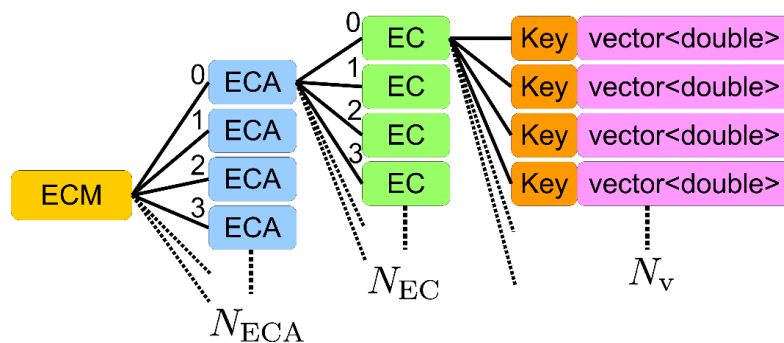

Figure 23. Structure of the ElementContainer (EC) family defined in the framework. The number of vectors, EC and ElementContainerArray (ECA) in an EC, ECA and ECM are N_v, N_{EC} and N_{ECA}, respectively.

Standard File Format: NeXus

We decided that the standard data file format at MLF should be NeXus, and an interface between data containers and NeXus file is prepared in the framework. A simple data file structure in NeXus format was designed in 2016. An interface between the EC family and NeXus files was developed by using the HDF5 C-API library. The rates of reading and writing ECMs from/to NeXus files with the interfaces were obtained and shown in Table 3. The file sizes on the disk are 4.0 and 1.3 gigabytes at $(N_v, N_{EC}, N_{ECA}) = (3,100,300)$ and $(3,10000,1)$, respectively. The data structures and dimensions of the former and latter datasets are the same as those of the three-dimensional histogram data produced by the chopper spectrometer and the powder diffractometer working at MLF. The efficiency of the interface is good enough but we should concern ourselves with how to increase the efficiency of data input/output in the framework, because the size of data files handled by the framework is increasing as the intensity of proton beam producing pulsed neutron beams increases. In future, we will improve the interface with multi-thread or network-distributed-parallel processing. Histogram data with their metadata in the NeXus format can be shared with other facilities around the world using NeXus-API or the HDF5 library.

Table 3. The efficiency of reading and writing NeXus files from/to the ElementContainerMatrices (ECMs). T_w and T_r are the writing and reading times in seconds with the interface. N_v, N_{EC} and N_{ECA} indicate the dimensions of ECM.

N_v	N_{EC}	N_{ECA}	T_w	T_r
3	100	300	24.7	8.33
3	10,000	1	10.39	2.76

Utsusemi, the Base Software for Data Reduction and Visualization at MLF

Overview of Utsusemi: Utsusemi is the software series used to analyze and visualize the neutron scattering data observed at MLF [56]. MLF adopted an event recording method for the DAQ system that records events including the time of flight and the position of the neutron detection. This method gives MLF users higher flexibility and efficiency for measurement and analysis. In event recording, the role of software is very important. The development of Utsusemi started from the software development for the chopper-type neutron inelastic measurement, which includes the device control system, data analysis, and visualization. These development products were utilized in actual user measurements at the chopper spectrometers at MLF, while we were proceeding with development of effective analysis for event recording data. In particular, we successfully contributed to the realization of the Multi-E_i method for inelastic scattering for the first time in the world [39]. As the other beamlines also required event-recording analysis, we made the data reduction and visualization parts in Utsusemi independent of the original to give it greater transferability as universal analysis software at MLF. We also produced additional packages based on Ustsusemi for each beamline. As a result, Utsusemi is introduced in a lot of beamlines at MLF to become one of the frameworks for data reduction and analysis.

Utsusemi software is written in C++, based on the Manyo Library framework and Python. All main functions are included in C++ codes for the processing speed and can be used from the Python interface. Utsusemi also has the GUI written in Python code and uses Python libraries. Because the user interface of Utsusemi is unified in Python, it is easy for users to make new functions or analysis procedures tailored to users' specific needs with Utsusemi commands.

Utsusemi software has already been distributed to many users at MLF with a release number. However, we think the current Utsusemi has a lot of functions that need to be improved or developed, so we continue to deliver the updated one with a short span, the so-called rolling release concept. For this release concept, we have a plan to build a portal site for the MLF computational environment group and a download page to distribute our updated software, including Utsusemi.

Data Reduction for Event-Recording: The most important function of Utsusemi is conversion from event-recording data produced from the MLF DAQ system to histogram data for easy understanding and visualization of the measurement results. This conversion function is very flexible. Using the information of event data like TOF, position of neutron detections, and absolute time, users can make histogram data from any TOF range and time region from measurement data. This enables users to easily measure the time-transient phenomena of the sample. For example, this function is used for a data reduction of an in situ neutron diffraction measurement during time-dependent temperature and tensile stress control, so called thermo-mechanical simulation (see Figure 8 of [57]). In addition, we successfully developed a DAQ electric module, TrigNET, which records common electric signals as events. By analyzing TrigNET events connected with instruments and SE equipment, neutron events can be filtered for each condition. We have already achieved this advanced method in the actual experiment and analysis on Utsusemi, and we provided this for users—for example, the measurement of the sample under a pulsed magnetic field and periodical electric field. Another example is a stroboscopic data reduction of the measurement of piezoelectric material under a cyclic electric field [58]. The Utsusemi event conversion supports most types of detectors utilized at MLF—for example, ^{3}He gas position sensitive detector, 1D- and 2D scintillation counters, and so on.

Recently, we succeeded in adding a differential event data reduction function to enable quasi-real-time analysis. During the measurement, the DAQ system continuously stores measured event data as binary files on a hard disk. This function only reads the difference between current binary files and previously read ones, with an interval time to be converted to histograms. Using the differential data, users can see the real-time change in measured data using visualization. Because this differential data format is the same as that of static event data, the analysis codes can also be unified between the two methods. This method has already been introduced in many beamlines to help users.

Command Sequence Execution: This software, named Sequence Editor, can be accessed via a GUI (Figure 24) and helps users to make procedures for executing analysis commands. Users can make their own command sequences to execute data reduction and visualization in this software. Commands are prepared by the instrument staff. Arguments for selected commands can be changed freely by editing the text boxes at the bottom of the window. These argument boxes are dynamically constructed according to a selected command. By pushing the Start button, the Sequence Editor executes a command sequence, step by step. If any error occurs in executing a command or the process is interrupted by the Stop button, the process stops but this software keeps all the parameters. All resulting data from the commands are kept in memory until they are deleted and users can directly send data to visualization software from the Sequence Editor. In addition, the command sequence made by users can be saved as a Python script to be executed directly on the console. If required, users can run the script directly in the Utsusemi environment or improve the saved script for their own analysis.

Visualization: Visualization software helps users to see and check any data at each data reduction step, from a simple TOF data to multi-dimensional data, i.e., $S(Q, E)$, measured by inelastic neutron scattering instruments. Utsusemi visualization software mainly consists of 1D-plotter (*X* and *Y* axes), 2D-plotter (*X*, *Y* axes and the intensity), PSD map visualization, and the data slicing software for multi-dimensional space data for a single crystal sample. These plotters can be controlled through the GUI or command-line on Python.

1D-Plotter, named MPlot, is usually used just to plot several histograms stored in data containers. This plotter has several basic functions such as changing types of lines and markers, scaling plot region, import/export of any text data, and so on. 2D-Plotter, named M2Plot, can plot two-dimensional data like the powder/grassy samples $S(Q, E)$ data and the sliced multi-dimensional data of a single crystal sample. VisualContM software treats multi-dimensional data $S(Q, E)$ obtained by a single crystal measurement This software makes $S(Q, E)$ data from the $S(phi, E)$ data produced from each detector histogram using sample information, i.e., the lattice parameters and the orientation against the incident beam. VisualContM has data slice functions to send the sliced data to M2Plot to visualize. We also

produced another kind of multi-dimensional slicing software that combines several tens of datasets measured at different orientations of a single crystal sample to cover a wider area in *Q*-space, which is useful for a 3D spin system. This software, named D4matSlicer, merges a series of datasets into one *S*(*Q*, *E*) data matrix and enables us to slice it.
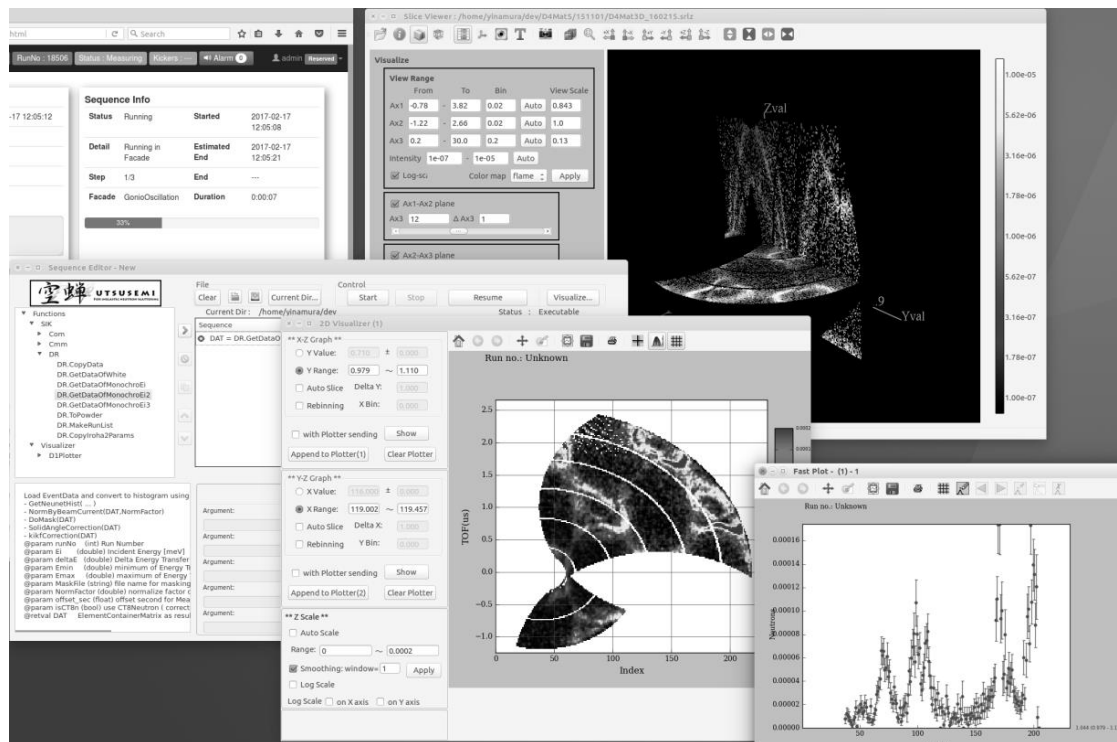

Figure 24. A screenshot of Utsusemi running.

Usability Improvement: General users have had difficulty installing and using Utsuemi on their own PCs until recently because the software and codes run only on Linux OS. This means that users must construct a Linux environment before using our software. Such a complex installation hinders the users' ability to analyze data at their offices and quickly prepare their results. To solve this problem, we produced a binary application and installer software executable on Windows and Mac OS. The binary installers are easy to use because they follow a regular way to install an application into each operating system (OS) and include all binary applications of Utsusemi, including Manyo Library, with the required software libraries. They work on 64-bit Windows 7, 8.2, and 10, or Mac OS 10.10 (Yosemite) and 10.11 (El Capitan).

Remote Access Framework, Nokiba and Shigure: At MLF, a remote access system is under development and partly in the test phase. The remote access system that we are developing aims to make it possible for remote users to process data. For system flexibility, our remote access system consists of two separated systems. One is a web interface that is used through the web browser and the other is a processing backend. The web interface is named Nokiba. Nokiba is a server-side program written in Python and run with a web server. The processing backend is Shigure. In typical usage, users can send commands to Shigure through the Nokiba web interface. Nokiba and Shigure are tied with a network connection and communicate with AMQP. AMQP is an abbreviated form of Advanced Message Queuing Protocol, which is used for message queueing and routing.

Shigure works under the publish-and-subscribe (pub/sub) model with AMQP. The pub/sub model is an asynchronous messaging paradigm. In that model, a sender of message does not know the implementation of receiver(s). In the pub/sub model of Nokiba and Shigure, users make commands for processing and send the commands to the Shigure backend through the Nokiba web interface.

The server side of Nokiba sends the message to the message broker over AMQP. In this scheme, the Nokiba server acts as a client (publisher) in the Shigure pub/sub model. Subscribers to Shigure can process Python script. One benefit of the pub/sub model is its flexibility. This loose coupling of Nokiba and Shigure enables us to adjust processes depending on the number of users or processes. This means it can start at a small scale and later increase in stages.

In the first stage of Nokiba and Shigure, data reduction with Utsusemi can be done through a web browser. Now we have developed a web user interface in prototype and Utsusemi can run on the Shigure backend. We started on improvement of the stability of the pub/sub implementation. On the other hand, this type of remote processing system has already been implemented in commercial cloud services (e.g., Amazon Web Services, Google Cloud Platform, etc.) and the utilization of such a commercial cloud will be beneficial for the reduction of costs and manpower. We are implementing the system in the cloud services for reviewing.

Issues with the Data Reduction Software: As described above, our data reduction software has been steadily developed to reach a high quality. However, many problems remain to be solved. One is the lack of advanced data correction functions—for example, the calculation of instrument resolution for obtained data, the correction for the neutron absorption process, the multi-scattering process, and the multi-phonon process at the sample. Another is the insufficiency of the software optimized to the target science for each beamline. Since the Manyo Library and Utsusemi provide the framework for the data reduction and include many common functions, we must prepare software suitable to users and their target science. Though users require these problems to be resolved, we cannot assign enough persons to these developments. For the sake of human resources, we have considered making collaborator members responsible for the beamline or allowing expert users to support software development. On the other hand, since some beamlines have produced original software for their own purposes, the effective management of such software is also an important issue.

In addition, as the intensity of MLF neutron source increases, the data size obtained in users' experiments becomes larger. We are afraid, therefore, that it will take too long to handle so much data. This technical problem takes a long time to solve. Our group must decide our priorities on the issues of software development and show our developments plan and schedules over the next few years.

3.1.4. Experimental Database: MLF EXP-DB

Overview of Experimental Database

At MLF, a large amount of experimental data is being produced in rapid succession with high-intensity beams. The typical data size produced in one experiment ranges from several tens of MB to several hundred GB in accordance with instruments and experiments, and the total amount of data generated annually in a whole facility at full performance is on the order of PB. Therefore, data management is an urgent issue for the facility and instrument staff. It is required to safely and efficiently store these data with limited storage resources over a long duration, and furthermore promote the acquisition of scientific results using them. Therefore, the access to and download of measurement logs (experimental metadata) and experimental data is also quite important for facility users. In order to meet these requirements, data should be centrally managed in a unified data repository in the facility, and rapid and effective data access should be provided to facility users. For those reasons, we have developed an integrated data management system, called MLF Experimental database (MLF EXP-DB), as a core system of our data management infrastructure [59]. The data policy of MLF is, that the experimental data will be kept by the facility and open to users for a certain time frame (three years), but the system for opening the data has not been implemented yet.

MLF EXP-DB

The system aims to deliver advanced services for data management and data access at MLF. To develop the system, we have employed Java-based commercial middleware with an XML database

system provided by Quatre-i Science Ltd., (Kyoto, Japan), named R&D Chain Management System Software. This middleware is based on a three-layer architecture model and consists of three main components: RCM-Web, RCM-Controller, and RCM-DB. These components all adopt XML technology, so that the middleware has flexibility and extensibility for data structure, workflow, and display output. Since data can have various structures at MLF according to instruments and experimental conditions using various SE equipment (experimental metadata), flexibility is necessary for handling such unstructured and semi-structured data. Moreover, extensibility makes it possible to meet future changes in system requirements. The experimental metadata will be collected through IROHA/IROHA2 and related business database such as proposal, sample, and so on. The main features of the system are as follows:

- Data cataloging: automatically correcting experimental data from instruments and creates the data catalog, which includes information on the paths of data files, samples, measurement conditions, and experimental proposals.
- Central data management: managing data file reposition. It processes the data transfer from instrument local storage to the unified data repository in the facility, archiving for long-term storage and on-demand retrieve.
- Database Link: correcting associated information on experiment such as experimental proposal, primary investigator, and chemical safety of samples by the database link to other business database systems.
- Web portal: providing the interface for data management and data access to facility staff and users via web portals. It is possible to manage, search, and download experimental data in these portals.

Reliability

Recently, we have improved the system, enhancing reliability toward the full-scale operation of the system and facility in the future. In the full-scale operation, the system is required to meet a dramatic rise in data rate with beam intensity and instruments performance resulting in an increasing load of data collection. Additionally, the database becomes rapidly enlarged owing to structural information such as tags and attributes in XML, so that its analytical process becomes lengthier with the increasing number of users. In such a situation, the system is required to provide effective and rapid data access to a large number of facility users, which is estimated to reach 10,000 annually. Therefore, the following three requirements should be satisfied [60]:

1. High reliability is required for a core system; however, the conventional system runs on a single physical server. By removing the single point of failure, service outages should be avoided as much as possible.
2. Scalability for data collection is required to accept the load for data collection increasing with instrument performance and beam intensity. However, the conventional system, which is a single integrated server, does not have such scalability.
3. A web portal enabling effective and quick data access should be provided to facility users. A data search function is especially important to find data for analysis from a large amount of data.

To address these issues, we redesigned the system and improved the web portal as follows:

- High availability: we improved the system as a redundant distributed system in a switch-over relationship. It is possible to perform a continuous data collection and provide stable data access in this configuration against system failure and service outage.
- Scalability: we redesigned the system to a scaled-out configuration enabling data collection load balancing and partitioning of bloating database. The improved system comprises two physical nodes. This architecture enables us to scale performance by adding nodes responding to the data rate.

- Usability: we improved the web portal for data access by implementing a flexible data search function. Users can search data with various conditions such as experimental proposal, sample, device conditions, etc.

Status of Operation

Currently, data management using the system is being performed on a trial basis with some instruments, i.e., BL02, BL11, BL17, and BL18 at MLF. In this trial operation, the data produced by previous experiments are primarily collected to accumulate metadata and verify the required information in the data catalog. We plan to start a full-scale operation soon. For data access, the basic development of the web portal has been completed. We will begin a trial of the web portal and remote access from outside the facility.

4. Sample Environment

The high penetrability of neutrons into materials enables us to prepare various kinds of sample environments (SE) to apply specific experimental conditions. Thus, sample environments are very important, especially for the neutron scattering technique. Typical sample environments used in neutron scattering experiments range from low temperature (up to several mK) to high temperature (up to 1873 K), steady magnetic environments to 10 T and their combination. These sample environments are widely used both in neutron diffraction experiments to determine the structures (atomic arrangements) of materials and in inelastic neutron scattering experiments to study elementary excitations, etc. of materials. On the other hand, there is another type of sample environment that has a dedicated purpose and usage. For example, a load frame to apply stress into a specimen to perform in situ neutron diffraction experiment under stress for studying mechanical properties is such a sample environment.

The strategy for introducing and operating in various sample environments at MLF is as follows: an official SE team is organized for commonly used SE, while an individual neutron instrument group develops and installs dedicated SE. The sample environment team provides technical support to individual neutron instrument groups.

In this chapter, we describe the status of the sample environments at MLF.

4.1. SE Equipment Available at MLF

The SE team is organized to operate and perform maintenance and development on the common SE equipment at MLF. The team consists of JAEA, KEK, and Comprehensive Research Organization for Science and Society (CROSS) staff, who all work together [61,62]. Two kinds of SE equipment are defined at MLF. One is the common SE equipment belonging to the SE team; the other is dedicated SE equipment belonging to individual beamline groups. High-cost SE equipment, high-performance SE equipment and standard SE equipment are the common types. Examples are a high magnetic field system, a dilution cryostat, and a standard cryostat. On the other hand, standard SE equipment such as a 10 K cryostat and special equipment such as a load frame to use in situ neutron diffraction under stress to study the deformation behavior of materials are defined as dedicated SE equipment. Furthermore, the SE team has determined and provided guidelines at MLF for designing the instruments and SE equipment; these are called SE protocols [61]. Basically, various pieces of SE equipment belonging to individual beamlines are designed according to the guidelines. The benefit of beamline groups adopting SE protocols is that the SE team can easily support the operation and maintenance of SE equipment. Furthermore, the SE equipment can be used among several beamlines, responding to experiment contents. Available common SE equipment by category of SE is shown in Table 4 [62]. Basically, these apparatuses were introduced after consideration of MLF staff, taking into account user requests at various user meetings, etc. First of all, cryogenic and magnet SE equipment to use in both elastic and inelastic neutron scattering experiments is well supported at MLF. There are two furnaces on high-temperature SE. One of them is a niobium wire furnace that can be operated up to 1873 K.

There is SE equipment to study soft matter properties by in situ small angle neutron scattering (SANS) experiments. One is a rheometer; the other is a gas and vapor adsorption measurement instrument. These are also used in offline characterization of samples. Although there is a dedicated High Pressure Neutron Diffractometer (BL11) at MLF, versatile high-pressure SE equipment is available to use at another beamlines. As characteristic SE equipment, light irradiation SE equipment that enables us to study photo-induced phenomena during in situ experiments is also available.

Table 4. Available common sample environment (SE) equipment at MLF.

Category of SE	Available Common SE Equipment
Cryogenic and Magnet	top-loading ^{4}He cryostat 1, bottom-loading ^{3}He cryostat 1, DR insert 1, superconducting magnet 1
High Temperature	furnaces 2 (niobium/Kanthal wire)
Soft Matter	rheometer 1, gas and vapor adsorption measurement instrument 1
High Pressure	Paris-Edinburgh press 1
Light Irradiation	xenon lamp light source 1

The neutron/muon experimental facility at MLF includes two experimental halls. The SE area, which is a dedicated working space for SE equipment to develop, calibrate, and perform maintenance, is prepared in both experimental hall No. 1 and No. 2. Furthermore, there are several rooms for SE equipment in the J-PARC research building, which is a nonradioactive controlled area.

Various dedicated SE equipment belonging to individual beamlines is shown in Table 5 [62]. The first feature of the dedicated SE equipment is that whether it is elastic neutron instruments (BL08, BL15, BL17, BL18, BL20, BL21) or inelastic neutron instruments (BL01, BL02, BL12, BL14), there are many standard cryostats (refrigerators). The second feature is that there is special purpose SE equipment. There are many SE apparatuses to apply high pressure into samples in BL11. SE equipment to study deformation process is introduced in BL19, which is an Engineering Materials Diffractometer. The hydrogen absorption/desorption measurement system is available in BL21, which is a High-Intensity Total Diffractometer originally designed to study hydrogen storage materials.

Table 5. Available SE Equipment Belonging to Individual Beamline Groups.

Instrument (BL)	SE Equipment and Specifications
4SEASONS (BL01): 4D-Space Access Neutron Spectrometer	top-loading GM CCR, high-temperature stick
DNA (BL02): Biomolecular Dynamics Spectrometer	cryofurnace
iBIX (BL03): IBARAKI Biological Crystal Diffractometer	gas flow type cooling system, 3-axis goniometer
ANNRI (BL04): Accurate Neutron-Nucleus Reaction Measurement Instrument	auto sampler
NOP (BL05): Neutron Optics and Fundamental Physics	Doppler shifter, XY moving stage
SuperHRPD (BL08): Super High Resolution Powder Diffractometer	top-loading GM CCR, bottom-loading GM CCR, vanadium furnace, auto sample changer
SPICA (BL09): Special Environment Neutron Powder Diffractometer	auto sample changer
NOBORU (BL10): NeutrOn Beamline for Observation & Research Use	5-axis compact goniometer
PLANET (BL11): High Pressure Neutron Diffractometer	temperature control system (for high pressure), Paris-Edinburgh press, 6-axis multi-anvil press, pressure control system 2, vacuum chamber glove box with pressure, ruby fluorescence measurement system, Raman spectrometer
HRC (BL12): High Resolution Chopper Spectrometer	bottom-loading GM CCR, ^{3}He circulation-type refrigerator
AMATERAS (BL14): Cold-Neutron Disk-Chopper Spectrometer	top-loading GM CCR, high-temperature stick, bottom-loading GM CCR

Table 5. *Cont.*

Instrument (BL)	SE Equipment and Specifications
TAIKAN (BL15): Small and Wide Angle Neutron Scattering Instrument	sample changer, bottom-loading GM CCR 2, laser heating apparatus, electromagnet 2 (one is shared with SHARAKU)
SOFIA (BL16): Soft Interface Analyzer	laser heating stage, Langmuir trough, heater state, Peltier element stage, solid/liquid interface cell with solenoid valve option
SHARAKU (BL17): Polarized Neutron Reflectometer	4K CCR, electromagnet (shared with TAIKAN), gas-atmosphere sample cell, humidity-control cell
SENJU (BL18): Extreme Environment Single Crystal Neutron Diffractometer	bottom-loading GM CCR, bottom-loading pulse tube CCR, RT goniometer
TAKUMI (BL19): Engineering Materials Diffractometer	loading machine 3 (RT, cryogenic, high temperature), furnace system for high temperature, loading machine, 100 K cooling system for loading experiment, fatigue machine, dilatometer, Eularian cradle, Gandolfi goniometer
iMATERIA (BL20): IBARAKI Materials Design Diffractometer	auto sample changer, sample changer 2, CCR, cryofurnace, ^{3}He circulation-type refrigerator, vanadium furnace
NOVA (BL21): High Intensity Total Diffractometer	sample changer, temperature-controlled sample changer, top-loading GM CCR, high-temperature stick, hydrogen absorption/desorption measurement system
RADEN (BL22): Energy Resolved Neutron Imaging System	sample stage (large, middle, small), high temperature system

BL: Beamline; GM: Gifford-MacMahon; CCR: closed-cycle refrigerator

Detailed information about the SE equipment at MLF can be obtained from the J-PARC homepage [63]. Furthermore, users may bring their own SE equipment to use during experiments at MLF, because many kinds of experiment can be conducted due to the world-class neutron-instruments and high intensity. In this case, before the actual use of equipment, a safety examination is performed by the safety examination team, which consists of JAEA, KEK, and CROSS staff.

4.2. Development of Pulsed Magnet System

It is important to open up opportunities for new experiments that could be performed at high-intensity neutron scattering facilities such as MLF. One example is to study various quantum materials at higher magnetic fields. Therefore, a higher magnetic field device is desirable.

The magnetic field is one typical sample environment in neutron scattering experiments to study magnetic structures and magnetic excitations in various materials. Usually, steady magnetic field environments of several types, for example, horizontal magnetic field equipment and vertical magnetic field equipment, are available in neutron scattering facilities. On the other hand, in spite of the importance of the magnetic field environments, if we plan to construct a steady higher magnetic field system, usually the strengths of those magnetic field environments are limited, because there is a technical problem about high electric power consumption, which means that running costs are high. Therefore, the typical accessible strengths of such conventional magnetic field equipment are approximately more than 10 and less than 20 T. Of course, a special dedicated higher steady magnetic field system of 26 T was constructed at Helmholtz-Zentrum Berlin (HZB, Berlin-Wannsee, Germany) [64,65].

One possible solution to overcome this situation is to adopt a pulsed magnetic field environment. The pulsed magnetic sample environment for neutron diffraction was developed in the 1980s by a Japanese group [66,67]. Now, we have been developing a pulsed magnetic system to achieve up to 30 T by collaboration with the group [68]. The features of the equipment include its compactness and portability, which enable it to be used with both elastic and inelastic neutron instruments. The final goal of the system is to achieve a variable duration time and a variable magnetic field. The developed pulsed magnet system consists of three parts: a capacitor bank power supply, a small solenoid coil (see Figure 25), and a cryostat insert. We describe each component of the equipment that composes the system. Performance testing of the fully assembled system started in 2016.

4.2.1. Capacitor Bank Power Supply

The developed capacitor bank power supply is shown in Figure 25a and the specifications are listed in Table 6. The most important parameters are the pulse width of the generated current and the repetition rate. The pulse width of the current is 2.65 ms at 50% of peak; the current profile is also shown in Figure 26. The repetition rate is one pulse per several minutes, because it takes several minutes to cool the solenoid coil by liquid nitrogen. The dimensions of the housing are 760 mm width by 1000 mm length by 1410 mm height. The weight is approximately 400 kg, which allows operators to transport it between individual beamlines by themselves.

Table 6. Basic Specifications of Capacitor Bank Power Supply.

Maximum Charging Energy	Maximum Charging Voltage	Charging Time	Maximum Output Current	Pulse Width	Repetition Rate
16 kJ	2 kV	about 30 s	8 kA	2.65 ms (at 50% of peak)	one pulse per several minutes

4.2.2. Small Solenoid Coil

The developed small solenoid coil is shown in Figure 25b. The shape of the coil is a hollow cylindrical shape, and its dimensions are 33 mm outer diameter by 12 mm inner diameter by 16 mm height. The round wire of the coil is made of a high tensile strength CuAg alloy and its diameter is 1 mm. The inductance and resistance of the assembled coil are 225 µH and 71 mΩ at 77 K, respectively. The lifetime is essentially determined by the insulation breakdown of the wire covering. The insulation of the many coils does not break down more than 1000 pulses.
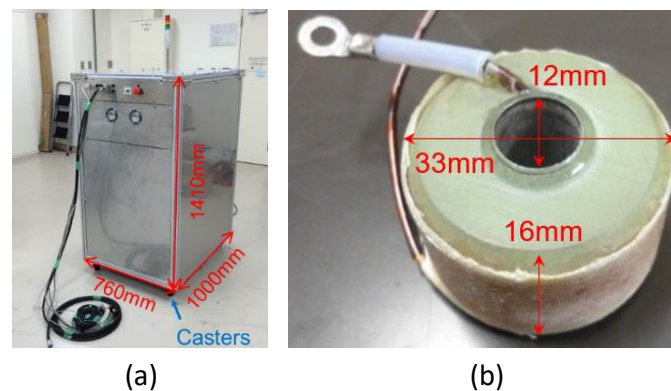

(a) (b)

Figure 25. Components of developed pulsed magnet system: (**a**) Capacitor bank power supply; (**b**) small solenoid coil.
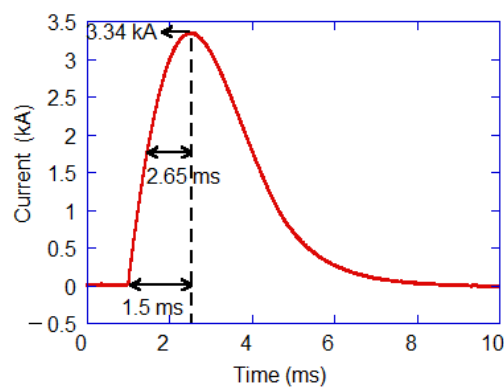

Figure 26. Current profile of the developed coil.

4.2.3. Cryostat Insert

The developed coil is inserted into a cryostat to use in neutron diffraction experiments. We fabricated the cryostat insert for the standard liquid helium flow cryostat, denoted Orange-cryostat (manufactured by AS Scientific Products Ltd, Oxfordshire, UK) with a 70 mm bore, which is one of the typical cryostats used in neutron experiments. The coil is immersed in liquid nitrogen and cooled at 77 K in order to decrease the resistance of the coil and remove the Joule heat generated by the pulsed current flow. A sample is cooled to approximately 1.5 K through helium gas. The maximum scattering angle is 30.6°. Using the developed pulsed magnetic system, test experiments were started, and it will be offered for user experiments in a couple of years.

5. Conclusions

In this paper, we have reported the developmental status of neutron devices, computational environments, and sample environments at MLF. As neutron devices, neutron detectors, optical devices including supermirror devices and ^{3}He neutron spin filters, and choppers are developed and installed at MLF. Neutron detectors used at MLF are PSDs, scintillation detectors, and gas-based two-dimensional detectors. In order to control a large number of commercially available PSDs, a readout system employing a high-speed network has been developed. Special scintillation detectors and gas-based two-dimensional detectors were also developed and installed at MLF. The supermirror devices such as neutron guides and focusing devices were developed at MLF using the IBS technique. Neutron guides with high reflectivity and large critical angle fabricated by the IBS technique were successfully installed in inelastic scattering instruments such as BL01, BL02, and BL14. In order to establish high neutron polarization using ^{3}He neutron spin filters, compact laser optics with a volume holographic grating element and a flexible non-magnetic heater have been developed for an in situ spin-exchange optical pumping application. The heater can be utilized in other applications where magnetic field disturbances are to be avoided. Developed and installed choppers at MLF are T0 choppers, Fermi choppers, and Disk choppers. These choppers are used at MLF for the purpose of background noise reduction, monochromatization of neutron beam, and elimination of undesired neutron or avoidance of frame overlap.

As for the computational environment, we have developed and equipped four software components, instrument control, data acquisition, data analysis, and a database. As instrument control software, IROHA was developed first and has now been upgraded to IROHA2. The event data recording method is employed as a standard data acquisition mode for neutron signal, conditions of sample environment equipment, status of beamline optical components, and so on. The MLF computational group has developed a software framework, Manyo Library, working on the 16 instruments for developing data reduction and analysis software. Consequently, Utsusemi software has been developed to analyze and visualize the data obtained via MLF instruments. We have also developed an integrated data management system named MLF Experimental database (MLF EXP-DB). These developments, including a remote access system are, however, still ongoing toward a higher throughput computational environment.

As for sample environment (SE) at MLF, the special SE team is organized to operate, perform maintenance, and develop common SE equipment at MLF. Consequently, a wide variety of common SE equipment is available at MLF to realize extreme sample conditions such as high and low temperatures and high magnetic fields, in addition to SE equipment belonging to individual beamline groups. This categorization enables us to expend minimum effort on operations and maintenance. The challenge of achieving a higher magnetic field is ongoing.

Author Contributions: The draft of Section 2.1 was prepared by S.S., T.S., Ka.S., T.N., K.T. and H.Y., Section 2.2 by K.So., D.Y., R.M., Section 2.3 by T.Ok., T.In., H.K., H.H. and Ke.S, Section 2.4 by S.I., K.Su, W.K., R.K., K.N., K.Sh. and M.N., Section 3 by T.Ot, T.N., Y.I., J.S., T.It., N.O. and K.M., Section 4 by K.A., S.O.-K. and M.W. Compilation of entire draft into the final version was made by Ka.S.

Conflicts of Interest: The authors declare no conflict of interest.

References

1. Satoh, S.; Muto, S.; Kaneko, N.; Uchida, T.; Tanaka, M.; Yasu, Y.; Nakayoshi, K.; Inoue, E.; Sendai, H.; Nakatani, T.; et al. Development of a readout system employing high-speed network for J-PARC. *Nucl. Instrum. Methods Phys. Res. A* **2008**, *600*, 103–106. [CrossRef]

2. Uchida, T.; Tanaka, M. Development of TCP/IP Processing Hardware. In Proceedings of the 2006 IEEE Nuclear Science Symposium Conference Record, San Diego, CA, USA, 29 October–4 November 2006; pp. 1411–1414. [CrossRef]

3. Sakasai, K.; Nakamura, T.; Katagiri, M.; Soyama, K.; Birumachi, A.; Satoh, S.; Rohdes, N.; Schooneveld, E. Development of neutron detector for engineering materials diffractometer at J-PARC. *Nucl. Instrum. Methods Phys. Res. A* **2008**, *600*, 157–160. [CrossRef]

4. Sakasai, K.; Toh, K.; Nakamura, T.; Harjo, S.; Moriai, A.; Itoh, T.; Abe, J.; Aizawa, K.; Soyama, K.; Katagiri, M.; et al. Development and Installation of Neutron Detectors for Engineering Materials Diffractometer at J-PARC. In Proceedings of the 19th Meeting on International Collaboration of Advanced Neutron Sources (ICANS-XIX), Grindelwald, Switzerland, 8–12 March 2010.

5. Nakamura, T.; Kawasaki, T.; Hosoya, T.; Toh, K.; Oikawa, K.; Sakasai, K.; Ebine, M.; Birumachi, A.; Soyama, K.; Katagiri, M. A large-area two-dimensional scintillator detector with a wavelength-shifting fibre readout for a time-of-flight single-crystal neutron diffractometer. *Nucl. Instrum. Methods Phys. Res. A* **2012**, *686*, 64–70. [CrossRef]

6. Kawasaki, T.; Nakamura, T.; Hosoya, T.; Oikawa, K.; Ohhara, T.; Kiyanagi, R.; Ebine, M.; Birumachi, A.; Sakasai, K.; Soyama, K.; et al. Detector system of the SENJU single-crystal time-of-flight neutron diffractometer at J-PARC/MLF. *Nucl. Instrum. Methods Phys. Res. A* **2014**, *735*, 444–451. [CrossRef]

7. Toh, K.; Nakamura, T.; Sakasai, K.; Soyama, K.; Hino, M.; Kitaguchi, M.; Yamagishi, H. Development of two-dimensional multiwire-type neutron detector system with individual line readout and optical signal transmission. *Nucl. Instrum. Methods Phys. Res. A* **2013**, *726*, 169–174. [CrossRef]

8. Toh, K.; Nakamura, T.; Sakasai, K.; Soyama, K.; Yamagishi, H. Evaluation of two-dimensional multiwire neutron detector with individual line readout under pulsed neutron irradiation. *J. Instrum.* **2014**, *9*, C11019. [CrossRef]

9. Mezei, F. Novel polarized neutron devices: Supermirror as spin component amplifier. *Commun. Phys.* **1976**, *1*, 81–85.

10. Soyama, K.; Ishiyama, W.; Murakami, K. Enhancement of reflectivity of multilayer neutron mirrors by ion polishing: Optimization of the ion beam parameters. *J. Phys. Chem. Solid* **1999**, *60*, 1587–1590. [CrossRef]

11. Maruyama, R.; Yamazaki, D.; Ebisawa, T.; Hino, M.; Soyama, K. Development of neutron supermirror with large-scale ion-beam sputtering instrument. *Physica B* **2006**, *385–386*, 1256–1258. [CrossRef]

12. Maruyama, R.; Yamazaki, D.; Ebisawa, T.; Hino, M.; Soyama, K. Development of neutron supermirrors with large critical angle. *Thin Solid Films* **2007**, *515*, 5704–5706. [CrossRef]

13. Wood, J. Status of supermirror research at OSMC. *Proc. SPIE* **1992**, *1738*, 22–29.

14. Maruyama, R.; Yamazaki, D.; Ebisawa, T.; Soyama, K. Development of high-reflectivity neutron supermirrors using an ion beam sputtering technique. *Nucl. Instrum. Methods Phys. Res. A* **2009**, *600*, 68–70. [CrossRef]

15. Maruyama, R.; Yamazaki, D.; Ebisawa, T.; Soyama, K. Effect of interfacial roughness correlation on diffuse scattering intensity in a neutron supermirror. *J. Appl. Phys.* **2009**, *105*, 083527. [CrossRef]

16. Kajimoto, R.; Nakajima, K.; Nakamura, M.; Soyama, K.; Yokoo, T.; Oikawa, K.; Arai, M. Study of the neutron guide design of the 4SEASONS spectrometer at J-PARC. *Nucl. Instrum. Methods Phys. Res. A* **2009**, *600*, 185–188. [CrossRef]

17. Nakajima, K.; Ohira-Kawamura, S.; Kikuchi, T.; Nakamura, M.; Kajimoto, R.; Inamura, Y.; Takahashi, N.; Aizawa, K.; Suzuya, K.; Shibata, K.; et al. AMATERAS: A Cold-Neutron Disk Chopper Spectrometer. *J. Phys. Soc. Jpn.* **2011**, *80*, SB028. [CrossRef]

18. Yamamura, K. Fabrication of Ultra Precision Optics by Numerically Controlled Local Wet Etching. *Ann. CIRP* **2007**, *56*, 541–544. [CrossRef]

19. Yamazaki, D.; Maruyama, R.; Soyama, K.; Takai, H.; Nagano, M.; Yamamura, K. Neutron beam focusing using large-m supermirrors coated on precisely-figured aspheric surfaces. *J. Phys. Conf. Ser.* **2010**, *251*, 012076. [CrossRef]

20. Yamazaki, D.; Nagano, M.; Maruyama, R.; Hayashida, H.; Soyama, K.; Yamamura, K. Neutron Focusing by a Kirkpatrick-Baez Type Super-mirror. *JPS Conf. Proc.* **2015**, *8*, 051009. [CrossRef]

21. Chupp, T.E.; Wagshul, M.E.; Coulter, K.P.; McDonald, A.B.; Happer, W. Polarized, high-density, gaseous ^{3}He targets. *Phys. Rev. C* **1987**, *36*, 2244–2251. [CrossRef]

22. Rich, D.R.; Gentile, T.R.; Smith, T.B.; Thompson, A.K. Spin exchange optical pumping at pressures near 1 bar for neutron spin filters. *Appl. Phys. Lett.* **2002**, *80*, 2210–2212. [CrossRef]

23. Moser, C.; Lawrence Ho, L.; Havermeyer, F. Self-aligned non-dispersive external cavity tunable laser. *Opt. Express* **2008**, *16*, 16691–16696. [CrossRef] [PubMed]

24. Liu, X.; Zhao, W.; Liu, H. Thermal Stress in High Power Semiconductor Lasers. In *Packaging of High Power Semiconductor Lasers*, 1st ed.; Springer: New York, NY, USA, 2015; pp. 89–105. ISBN 978-1-4939-5590-9.

25. Kissel, H.; Köhler, B.; Biesenbach, J. High-power diode laser pumps for alkali lasers (DPALs). *Proc. SPIE* **2012**, *824*, 82410Q. [CrossRef]

26. Hayashida, H.; Oku, T.; Kira, H.; Sakai, K.; Takeda, M.; Sakaguchi, Y.; Ino, T.; Shinohara, T.; Ohoyama, K.; Suzuki, J.; et al. Development and demonstration of in-situ SEOP 3He spin filter system for neutron spin analyzer on the SHARAKU polarized neutron reflectometer at J-PARC. *J. Phys. Conf. Ser.* **2014**, *528*, 012020. [CrossRef]

27. Kira, H.; Hayashida, H.; Iwase, H.; Ohishi, K.; Suzuki, J.; Oku, T.; Sakai, K.; Hiroi, K.; Takata, S.; Ino, T.; et al. Demonstration Study of Small-Angle Polarized Neutron Scattering Using Polarized ^{3}He Neutron Spin Filter. *JPS Conf. Proc.* **2015**, *8*, 036008. [CrossRef]

28. Walker, T.G. Fundamentals of Spin-Exchange Optical Pumping. *J. Phys. Conf. Ser.* **2011**, *294*, 012001. [CrossRef]

29. Babcock, E.; Nelson, I.; Kadlecek, S.; Driehuys, B.; Anderson, L.W.; Hersman, F.W.; Walker, T.G. Hybrid Spin-Exchange Optical Pumping of ^{3}He. *Phys. Rev. Lett.* **2003**, *91*, 123003. [CrossRef] [PubMed]

30. Tong, X.; Pierce, J.; Lee, W.T.; Fleenor, M.; Chen, W.C.; Jones, G.L.; Robertson, J.L. Electrical heating for SEOP-based polarized ^{3}He system. *J. Phys. Conf. Ser.* **2010**, *251*, 012087. [CrossRef]

31. Babcock, E.; Salhi, Z.; Theisselmann, T.; Starostin, D.; Schmeissner, J.; Feoktystov, A.; Mattauch, S.; Pistel, P.; Radulescu, A.; Ioffe, A. SEOP polarized ^{3}He Neutron Spin Filters for the JCNS user program. *J. Phys. Conf. Ser.* **2016**, *711*, 012008. [CrossRef]

32. Ino, T.; Hayashida, H.; Kira, H.; Oku, T.; Sakai, K. Non-magnetic flexible heaters for spin-exchange optical pumping of ^{3}He and other applications. *Rev. Sci. Instrum.* **2016**, *87*, 115108. [CrossRef] [PubMed]

33. Itoh, S.; Ueno, K.; Ohkubo, R.; Sagehashi, H.; Funahashi, Y.; Yokoo, T. T0 chopper developed at KEK. *Nucl. Instr. Methods Phys. Res. Sect. A* **2012**, *661*, 86–92. [CrossRef]

34. Kajimoto, R.; Nakamura, M.; Inamura, Y.; Mizuno, F.; Nakajima, K.; Takahashi, N.; Ohira-Kawamura, S.; Yokoo, T.; Maruyama, R.; Soyama, K.; et al. Commissioning of the Fermi-Chopper Spectrometer 4SEASONS at J-PARC—Background Study. In Proceedings of the 19th Meeting on International Collaboration of Advanced Neutron Sources (ICANS-XIX), Grindelwald, Switzerland, 8–12 March 2010.

35. Kajimoto, R.; Nakamura, M.; Inamura, Y.; Mizuno, F.; Nakajima, K.; Ohira-Kawamura, S.; Yokoo, T.; Nakatani, T.; Maruyama, R.; Soyama, K.; et al. The Fermi Chopper Spectrometer 4SEASONS at J-PARC. *J. Phys. Soc. Jpn.* **2011**, *80*, SB025. [CrossRef]

36. Fermi, E.; Marshall, J.; Marshall, L. A Thermal Neutron Velocity Selector and Its Application to the Measurement of the Cross Section of Boron. *Phys. Rev.* **1947**, *72*, 193–196. [CrossRef]

37. Itoh, S.; Ueno, K.; Yokoo, T. Fermi chopper developed at KEK. *Nucl. Instrum. Methods Phys. Res. A* **2012**, *661*, 58–63. [CrossRef]

38. Nakamura, M.; Nakajima, K.; Kajimoto, R.; Arai, M. Utilization of multiple incident energies on Cold-Neutron Disk-Chopper Spectrometer at J-PARC. *J. Neutron Res.* **2007**, *15*, 31–37. [CrossRef]

39. Nakamura, M.; Kajimoto, R.; Inamura, Y.; Mizuno, F.; Fujita, M.; Yokoo, T.; Arai, M. First Demonstration of Novel Method for Inelastic Neutron Scattering Measurement Utilizing Multiple Incident Energies. *J. Phys. Soc. Jpn.* **2009**, *78*, 093002. [CrossRef]

40. Nakamura, M.; Kajimoto, R. General Formulae for the Optimized Design of Fermi Chopper Spectrometer. *JPS Conf. Proc.* **2014**, *1*, 014018. [CrossRef]

41. Suzuki, J.; Murakami, K.; Manabe, A.; Kawabata, S.; Otomo, T.; Furusaka, M. Object-oriented data analysis environment for neutron scattering. *Nucl. Instrum. Methods Phys. Res. A* **2004**, *534*, 175–179. [CrossRef]

42. Yasu, Y.; Nakayoshi, K.; Sendai, H.; Inoue, E.; Tanaka, M.; Suzuki, S.; Satoh, S.; Muto, S.; Otomo, T.; Nakatani, T.; et al. Development of DAQ-Middleware. In Proceedings of the 17th International Conference on Computing in High Energy and Nuclear Physics (CHEP09), Prague, Czech Republic, 21–27 March 2009; p. 022025. [CrossRef]

43. Mcgreevy, R.; Otomo, T.; Anderson, I.; Miller, S.; Geist, A. New opportunities for data analysis software: An international Collaboration. *Neutron News* **2004**, *15*, 25–27. [CrossRef]

44. Nakatani, T.; Inamura, Y.; Ito, T.; Harjo, S.; Kajimoto, R.; Arai, M.; Ohhara, T.; Nakagawa, H.; Aoyagi, T.; Otomo, T.; et al. The Implementation of the Software Framework in J-PARC/MLF. In Proceedings of the 12th International Conference on Accelerator and Large Experimental Physics Control Systems, Kobe, Japan, 12–16 October 2009; p. 673.

45. Nakatani, T.; Inamura, Y.; Ito, T.; Otomo, T. Data acquisition and device control software framework in MLF, J-PARC. In Proceedings of the 21st Meeting of the International Collaboration on Advanced Neutron Sources (ICANS-XXI), Mito, Japan, 29 September–3 October 2014; p. 493. [CrossRef]

46. Nakatani, T.; Inamura, Y.; Ito, T.; Otomo, T. The Control Software Framework of the Web Base. In Proceedings of the 2nd International Symposium on Science at J-PARC, Tsukuba, Japan, 12–15 July 2014; p. 036013. [CrossRef]

47. Nakatani, T.; Inamura, Y.; Ito, T.; Moriyama, K. IROHA2: Standard instrument control software framework in MLF, J-PARC. In Proceedings of the New Opportunities for Better User Group Software NOBUGS2016, Copenhagen, Denmark, 17–19 October 2016; p. 76. [CrossRef]

48. Nakatani, T.; Inamura, Y.; Ito, T.; Otomo, T.; Satoh, S.; Muto, S.; Nakayoshi, K.; Sendai, H.; Inoue, E.; Yasu, Y. Event Mode Data Acquisition System at MLF/J-PARC. In Proceedings of the 19th Meeting on International Collaboration of Advanced Neutron Sources (ICANS-XIX), Grindelwald, Switzerland, 8–12 March 2010.

49. Nakatani, T.; Inamura, Y.; Moriyama, K.; Ito, T.; Muto, S.; Otomo, T. Event recording data acquisition system and experiment data management system for neutron experiments at MLF, J-PARC. In Proceedings of the 12th Asia Pacific Physics Conference (APPC12), Chiba, Japan, 14–19 July 2013; p. 014010. [CrossRef]

50. Uchida, T. Hardware-Based TCP Processor for Gigabit Ethernet. *IEEE Trans. Nucl. Sci.* **2008**, *55*, 1631–1637. [CrossRef]

51. Nakayoshi, K.; Yasu, Y.; Inoue, E.; Sendai, H.; Tanaka, M.; Satoh, S.; Muto, S.; Kaneko, N.; Otomo, T.; Nakatani, T.; et al. Development of a Data Acquisition Sub-System using DAQ-Middleware. *Nucl. Instrum. Methods Phys. Res. A* **2009**, *600*, 173–175. [CrossRef]

52. Nakayoshi, K.; Yasu, Y.; Inoue, E.; Sendai, H.; Tanaka, M.; Satoh, S.; Muto, S.; Suzuki, J.; Otomo, T.; Nakatani, T.; et al. DAQ-Middleware for MLF/J-PARC. *Nucl. Instrum. Methods Phys. Res. A* **2010**, *623*, 537–539. [CrossRef]

53. Yasu, Y.; Nakayoshi, K.; Sendai, H.; Inoue, E. Functionally of DAQ-Middleware. *IEEE Trans. Nucl. Sci.* **2010**, *57*, 487–490. [CrossRef]

54. Suzuki, J.; Nakatani, T.; Ohhara, T.; Inamura, Y.; Yonemura, M.; Morishima, T.; Aoyagi, T.; Manabe, A.; Otomo, T. Object-oriented data analysis framework for neutron scattering experiments. *Nucl. Instrum. Methods Phys. Res. A* **2009**, *600*, 123–125. [CrossRef]

55. Suzuki, J.; Inamura, Y.; Ito, T.; Nakatani, T.; Otomo, T. "Manyo-Lib" Object-Oriented Data Analysis Framework for Neutron Scattering. In Proceedings of the New Opportunities for Better User Group Software NOBUGS2016, Copenhagen, Denmark, 17–19 October 2016; p. 72.

56. Inamura, Y.; Nakatani, T.; Suzuki, J.; Otomo, T. Development status of software 'Utsusemi' for Chopper Spectrometers at MLF, J-PARC. *J. Phys. Soc. Jpn.* **2013**, *82*, SA031. [CrossRef]

57. Harjo, S.; Ito, T.; Aizawa, K.; Arima, H.; Abe, J.; Moriai, A.; Iwahashi, T.; Kamiyama, K. Current Status of Engineering Materials Diffractometer at J-PARC. *Mater. Sci. Forum* **2011**, *681*, 443–448. [CrossRef]

58. Kawasaki, T.; Ito, T.; Inamura, Y.; Nakatani, T.; Harjo, S.; Gong, W.; Iwahashi, T.; Aizawa, K. Neutron Diffraction Study of Piezoelectric Material under Cyclic Electric Field using Event Recording Technique. In Proceedings of the 21st Meeting of the International Collaboration on Advanced Neutron Sources (ICANS-XXI), Mito, Japan, 29 September–3 October 2014; pp. 528–531. [CrossRef]

59. Moriyama, K.; Nakatani, T. A Data Management Infrastructure for Neutron Scattering Experiments in J-PARC/MLF. In Proceedings of the 15th International Conference on Accelerator and Large Experimental Physics Control Systems ICALEPCS2015, Melbourne, Australia, 17–23 October 2015; p. 834.

60. Moriyama, K.; Nakatani, T. Recent Progress in the Development of MLF EXP-DB in J-PARC. In Proceedings of the New Opportunities for Better User Group Software NOBUGS2016, Copenhagen, Denmark, 17–19 October 2016; p. 80. [CrossRef]

61. Aso, T.; Yamauchi, Y.; Sakaguchi, Y.; Munakata, K.; Ishikado, M.; Ohira-Kawamura, S.; Yokoo, T.; Watanabe, M.; Takata, S.; Hattori, T.; et al. Present status of sample environment at J-PARC MLF. In Proceedings of the 21th International Collaboration on Advanced Neutron Source (ICANS-XXI), Mito, Japan, 29 September–3 October 2014.

62. Ohira-Kawamura, S.; Oku, T.; Watanabe, M.; Takahashi, R.; Munakata, K.; Sakaguchi, Y.; Ishikado, M.; Ohuchi, K.; Hattori, T.; Kira, H.; et al. Sample Environment at the J-PARC MLF. *J. Neutron Res.* **2017**, *19*, 15–22. [CrossRef]

63. J-PARC. Available online: http://j-parc.jp/researcher/MatLife/en/se/equipment.html (accessed on 27 July 2017).

64. Steiner, M.; Tennant, D.A.; Smeibidl, P. New high field magnet for neutron scattering at Hahn-Meitner Institute. *J. Phys. Conf. Ser.* **2006**, *51*, 470–474. [CrossRef]

65. Smeibidl, P.; Tennant, A.; Ehmler, H.; Bird, M. Neutron Scattering at Highest Magnetic Fields at the Helmholtz Centre Berlin. *J. Low Temp. Phys.* **2010**, *159*, 402–405. [CrossRef]

66. Nojiri, H.; Takahashi, K.; Fukuda, T.; Fujita, M.; Arai, M.; Motokawa, M. 25T repeating pulsed magnetic fields system for neutron diffraction experiments. *Physica B* **1998**, *241–243*, 210–212.

67. Nojiri, M.; Motokawa, H.; Takahashi, K.; Arai, M. 30 T repeating pulsed field system for neutron diffraction. *IEEE Trans. Appl. Supercond.* **2000**, *10*, 534–537. [CrossRef]

68. Watanabe, M.; Nojiri, H.; Itoh, S.; Ohira-Kawamura, S.; Kihara, T.; Masuda, T.; Sahara, T.; Soda, M.; Takahashi, R. Development of compact high field pulsed magnet system for new sample environment equipment at MLF in J-PARC. In Proceedings of the International Symposium of Quantum Beam Science at Ibaraki University, Mito, Japan, 18–20 November 2016.